PHOTOPROTECTIVE RESPONSE OF THE SEA ICE DIATOM *Fragilariopsis cylindrus* TO ULTRAVIOLET-B RADIATION UNDER ELEVATED TEMPERATURE AND LIGHT EXPOSURE

A thesis submitted in partial fulfillment of the requirements for the degree

MASTER OF SCIENCE

in

MARINE BIOLOGY

by

NICOLE LYN SCHANKE
MAY 2015

at

THE GRADUATE SCHOOL OF THE UNIVERSITY OF CHARLESTON, SOUTH CAROLINA AT THE COLLEGE OF CHARLESTON

Approved by:

Dr. Giacomo DiTullio, Thesis Advisor

Dr. Michael Janech

Dr. Gregory Doucette

Dr. Jill Johnson

Dr. Amy T. McCandless, Dean of the Graduate School

UMI Number: 1587032

UMI

Dissertation Publishing

UMI 1587032

ProQuest®

ABSTRACT

PHOTOPROTECTIVE RESPONSE OF THE SEA ICE DIATOM *Fragilariopsis cylindrus* TO ULTRAVIOLET-B RADIATION UNDER ELEVATED TEMPERATURE AND LIGHT EXPOSURE

A thesis submitted in partial fulfillment of the requirements for the degree

MASTER OF SCIENCE

in

MARINE BIOLOGY

by

NICOLE LYN SCHANKE
MAY 2015

at

THE GRADUATE SCHOOL OF THE UNIVERSITY OF CHARLESTON, SOUTH CAROLINA AT THE COLLEGE OF CHARLESTON

The destruction of the ozone layer, concomitant with a projected enhancement in ocean stratification, will increase the dosage of ultraviolet radiation (UVR), as well as sea surface temperature and incident light level. The diatom *Fragilariopsis cylindrus* and other Antarctic phytoplankton will therefore be exposed to, and require protection from, increasing levels of damaging UVR, under elevated temperatures and light conditions. It has been hypothesized that phytoplankton utilize photoprotective pigments and the production of mycosporine-like amino acids as strategies against UVB-induced production of reactive oxygen species (ROS). The goal of this research was to investigate photoprotective mechanisms employed by *F. cylindrus*, following exposure to enhanced UVB. Interactive effects of temperature and light level were explored, as cultures were subjected to temperatures of $0^{o}C$ or $4^{o}C$ and light levels of 15 $\mu E\ m^{-2}\ s^{-1}$ or 100 $\mu E\ m^{-2}\ s^{-1}$, in order to approximate current and future Southern Ocean stratification conditions. Growth rate and photosynthesis significantly declined by 40-80% and 50-90%, respectively, following exposure to high UVB relative to control conditions. This decline in physiological health was accompanied by a 50-300% increase in photoprotective mechanisms. Exposure to high UVB under current climate conditions resulted in the least amount of photodamage and photoprotection. Conversely, elevated light level resulted in the greatest decrease in growth and photosynthesis, accompanied with the greatest increase in photoprotection when exposed to high UVB. Under both light levels, the elevated temperature appeared to mitigate damage caused by high UVB exposure. The results of this study shed light on the mechanisms utilized by *F.cylindrus* in response to oxidative stress induced by UVB, and how these mechanisms may be expected to change under future ocean stratification conditions.

ACKNOWLEDGEMENTS

TABLE OF CONTENTS

LIST OF FIGURES AND TABLES

Introduction

Climate Change and the Southern Ocean

Several IPCC models are predicting a global increase in ocean stratification,

resulting from warming sea surface temperatures (SST) and increased fresh water input

(Capotondi *et al*., 2012; Sarmiento *et al*., 2004). High SST and low salinity decrease the

density of surface waters, and increase the density differential between surface and deep

water. Stratification results in a shallower mixed layer depth and limited entrainment of

nutrients across the pycnocline (Capotondi *et al*., 2012). Increased ocean stratification

reduces vertical mixing, causing the phytoplankton community, whose vertical

movements are dependent upon this circulation, to remain within the shallower mixed

layer. In these surface waters, the phytoplankton will be exposed to elevated average

temperature and light conditions, due to the increased solar radiation in the upper layers

of the water column and reduced vertical mixing rates.

Organisms inhabiting marine ecosystems are faced with a suite of environmental

challenges. These include changes in SST, salinity, nutrient availability, and light level,

as well as pollution from anthropogenic sources. One anthropogenic impact that has

especially affected marine organisms of the Antarctic ecosystem has been the

introduction of ozone-depleting compounds into the atmosphere. Chlorofluorocarbons

(CFCs), one of the several classes of ozone-depleting compounds, are used as

refrigerants, aerosol propellants, cleaning solvents and foaming agents in the

manufacturing of plastics (Rowland, 1989). These compounds have relatively long

residence times, often remaining in the atmosphere for 40 to 150 years (Rowland, 1989).

As our society has become more industrialized, large amounts of CFCs and similar

halogenated compounds have been released into the atmosphere, causing the formation of a hole in the ozone layer. The presence of this stratospheric ozone layer in the atmosphere is essential in reducing the amount of destructive ultraviolet radiation (UVR) that strikes the earth's surface. Therefore, the reduction in ozone levels results in an increased exposure to ultraviolet radiation.

Antarctica and the Southern Ocean are especially susceptible to increases in ultraviolet radiation as a result of the localization of ozone depletion within this region. The ozone hole appears over the South Pole in late austral winter (July) and remains until late spring (November) (Figure 1) (Díaz *et al*., 2000; Bettwy, 2003). The maximum annual stratospheric ozone loss occurs in late September, when complete depletion of ozone molecules can be found between 12 and 20 km above Antarctica's surface. In 2000, the ozone hole encompassed a record-breaking 28.3×10^6 km^2 (Bettwy, 2003). There are several factors that, when combined, give rise to a maximum ozone hole occurring over Antarctica. The major initiating factor is the anthropogenic input of CFCs (and other halogenated compounds) into the stratosphere. The presence of the Antarctic polar vortex isolates the stratosphere over Antarctica from the stratosphere of the lower latitudes, trapping CFCs and their resulting chloride atoms (Whitehead *et al*., 2000). Once the unstable chloride atoms are formed, a chain reaction is initiated, in which the chloride atoms destroy ozone (O_3) molecules (Rowland, 1989). During the Antarctic winters, temperatures drop to the lowest levels reached on Earth and polar stratospheric clouds form. These clouds contain ice crystals, which provide a surface for the conversion of CFCs into active chloride atoms (Bettwy, 2003). As the temperatures begin to increase in the austral spring, solar energy facilitates the formation of the reactive

chloride atoms, and ozone depletion begins (Díaz *et al.*, 2000). In the late austral spring to summer, warmer temperatures cause the ice crystals of the polar stratospheric clouds to melt, preventing the continued formation of active chlorine and halting the expansion of the ozone hole for the year.

Due to the annual presence of the Antarctic Ozone Hole, phytoplankton inhabiting Southern Ocean surface waters are expected to not only experience elevated temperature and light as a result of increased ocean stratification, but also increased levels of ultraviolet radiation (UVR) due to minimal amounts of ozone in the stratosphere. This allows a greater intensity of UVR to reach Earth's surface; however, this is dependent upon the wavelength of the radiation. For instance, destructive UVC radiation has relatively short wavelengths (200-280 nm) and is almost completely absorbed within the stratosphere. In contrast, UVA and UVB radiation have relatively longer wavelengths (320-400 nm and 280-320 nm, respectively) and are more able to pass through the atmosphere (Smith *et al.*, 1992). Nonetheless, it is ultimately the concentration of ozone in the stratosphere that determines the amount of UVB radiation that reaches the earth's surface. Without the protection of the ozone layer during the austral spring, Antarctic organisms are exposed to higher levels of damaging UVB radiation.

UVB radiation can be especially damaging to phytoplankton as it is able to penetrate up to 30 m in the open ocean water column (Kirk, 1994; Speekmann *et al.*, 2000). Nucleic acids absorb UVB radiation, which can result in genetic mutations and the inhibition of transcription (Vincent and Neale, 2000). UVB increases the production of reactive oxygen species (ROS), which induces deleterious effects upon photosynthetic parameters, lipids and cell membranes (Murphy, 1983; Vincent and Neale, 2000).

Specifically among phytoplankton, UVB has been shown to reduce primary production by inhibiting carbon uptake (by 25-50%) and bleaching pigments. UV radiation has also been shown to inhibit nitrogen uptake and metabolism, impair mobility, decrease growth rates (by 75-100%) and alter phytoplankton community composition (Vernet, 2000). In response to the many adverse impacts of ultraviolet radiation, marine phytoplankton have developed several types of photoprotective responses to combat the stressful production of ROS. For example, chromophytic phytoplankton (those containing chlorophyll c) can typically utilize photoprotective carotenoids and xanthophyll cycling, as well as the production of mycosporine-like amino acids as photoprotective strategies to combat ROS accumulation. The ability of phytoplankton species to employ these photoprotective mechanisms, while facing elevated temperature and light levels, would be highly beneficial as the Southern Ocean undergoes climactic changes.

Photoacclimation and Protective Pigments

After the absorption of light energy by chlorophyll *a* within the light harvesting complexes, the cell can deactivate this energy through one of several pathways. The majority of this energy is used to drive the photochemical reactions of photosynthesis. A small part of the energy is dissipated as heat or fluorescence. A still significant amount of this energy can be dissipated through the formation of the triplet-state excitation of chlorophyll *a* (^{3}chlorophyll *a**). Yet under high light stress, photosynthesis is at its maximum, and an increased amount of the absorbed energy has to be dissipated through fluorescence or ^{3}chlorophyll *a** formation. An elevated presence of ^{3}chlorophyll *a** within the cell can be especially detrimental, as it can react with oxygen to produce ROS

(Brunet *et al*., 2011). However, photosynthetic organisms have evolved the ability to photoacclimate to changes in their light field.

Photoacclimation is the process of optimizing cellular mechanisms, mainly growth and photosynthesis, in response to changes in irradiance. This often includes physiological changes that occur over the course of seconds to days (Brunet *et al*., 2011). One method of long-term photoacclimation involves changes in the relative amounts of pigments with differing functions. Pigments can be classified as photosynthetic, in which they function to transfer absorbed light energy to the reaction centers of the photosystems, or they can be classified as photoprotective, in which the pigments deactivate excited chlorophyll *a* and minimize ROS production (Brunet *et al*., 2011; Roy 2000). In chromophytes, like diatoms, the major pigments utilized in photosynthesis are chlorophyll *a* and c and fucoxanthin, while photoprotective pigments consist primarily of carotenoids such as, β-carotene, diadinoxanthin and diatoxanthin. Cells that have been acclimated to relatively high light levels tend to have higher cellular concentrations of photoprotective carotenoids and lower concentrations of photosynthetic pigments than cells that have been acclimated to lower light levels (Brunet *et al*., 2011).

One of the main short-term photoacclimation responses is activation of the xanthophyll cycle. Xanthophyll cycling enables unicellular phytoplankton to immediately (e.g. timescales of minutes) respond to changes in light exposure. When photosynthetic organisms absorb light, chlorophyll *a* molecules are excited to a singlet-state (Müller *et al*., 2001). The xanthophyll cycle allows excited chlorophyll *a* molecules to dissipate this energy to other pigments, like carotenoids (Falkowski & Raven, 1997), and minimize the production of singlet oxygen (Müller *et al*., 2001). In diatoms, dinoflagellates and

haptophytes, this cycling consists of a conversion between the carotenoids diadinoxanthin (DD) and diatoxanthin (DT), which is facilitated by the diadinoxanthin de-epoxidase enzyme within thylakoid membranes (Yamamoto, 1985; Moisan *et al*., 1998; Kropuenske *et al*., 2009) (Figure 1). When light intensity increases, the lumen within the thylakoid membranes becomes more acidic via proton transport. This drop in the intrathylakoid pH (~5.2), as well as the presence of ascorbate and monogalactosyldiacylglycerol lipids, enhances de-epoxidase activity, removing the epoxide from DD and producing DT, and thereby increasing the DT:DD+DT ratio (Figure 1). Conversely, under low light conditions, the pH increases (~7.5), enhancing the activity of the epoxidase enzyme in the stroma. This converts DT to DD, and decreases the DT:DD+DT ratio (Moisan *et al*., 1998). These reactions provide the organism with a less damaging way to dissipate excess energy from high light exposure, making the xanthophyll cycle a potential photoprotective mechanism.

The response of xanthophyll cycling following UVB exposure does not appear to be consistent across all phytoplankton groups. Certain species of diatoms, dinoflagellates and haptophytes, as well as natural phytoplankton communities, have shown an activation of the xanthophyll cycle following UVB exposure. Because one of the major targets of UV damage is photosystem II, the amount of light energy that this photosystem can use to drive photosynthesis is decreased. This decrease in light utilization to drive biochemical carbon fixation increases excess light energy and the probability of ROS formation. As a result, these phytoplankton species will activate the cycling of xanthophyll pigments by increasing the cellular concentration of the de-epoxidized pigment (diatoxanthin, or zeaxanthin in some chlorophyll *b* containing species), while the

6

concentration of the epoxidized pigment (diadinoxanthin, or violaxanthin in some chlorophyll *b* containing species) is reduced (Brunet *et al*., 2011). Conversely, xanthophyll cycling in several other diatom, haptophyte and chlorophyte species has been found to be inhibited by UVB. This inactivation was often caused by an increase in the epoxidase activity, converting diatoxanthin to diadinoxanthin, due to loss of the pH gradient across thylakoid membranes (Brunet *et al*., 2011; Mewes and Richter, 2002).

Mycosporine-like Amino Acids

Mycosporine-like amino acids (MAAs) are low molecular weight (LMW) compounds (usually less than 400 Da (Oren and Gunde-Cimerman, 2007)), consisting of a cyclohexenone or cyclohexenimine ring and a nitrogen-containing substituent (an amino acid, amino alcohol or amino group) (Callone *et al*., 2006). These LMW compounds have absorbance maxima ranging from 310 to 360 nm, which includes wavelengths in both UVA and UVB radiation. Currently, there are more than 20 MAAs that have been well studied, and new MAAs are still being identified as research in this field expands (Carreto and Carignan, 2011). Mycosporine-like amino acids are thought to be good sunscreen compounds due to their high photostability and high molar absorptivity (ε = 28,100 to 50,000 M^{-1} cm^{-1}) within UVR wavelengths (Shick and Dunlap, 2002). In response to UVB exposure, intracellular concentrations of MAAs have been shown to increase (Wood, 1989), which has also been correlated with decreased photoinhibition and photodamage (Vernet *et al*., 1994; Shick and Dunlap, 2002), suggesting that the production of MAAs is a viable photoprotective mechanism.

MAAs are produced through a side-branch of the Shikimate pathway (Shick *et al*., 1999) (Figure 2). The Shikimate pathway is responsible for the synthesis of the aromatic

amino acids phenylalanine, tyrosine and tryptophan, as well as folate cofactors and isoprenoid quinones (Shick and Dunlap, 2002). The compound 3-dehydroquinate (DHQ) is an intermediate within this pathway, and it is from this compound that the MAA-producing branch of the Shikimate pathway stems (Favre-Bonvin *et al*., 1987; Shick and Dunlap, 2002). Depending on which enzyme acts on DHQ, 3-dehydroquinate dehydratase or O-methyltransferase, this metabolic pathway branches to produce either aromatic amino acids or MAAs, respectively (Shick and Dunlap, 2002). O-methyltransferase is responsible for the production of gadusol from DHQ. A series of enzymatic conversions, driven by carbamoyl phosphate synthetase and ATP grasp ligase, alters gadusol to produce the entire suite of over 20 MAAs (Gao and Garcia-Pichel, 2011a; Rosic, 2012). This synthesis pathway has been recently studied in the cyanobacteria species, including *Anabaena variabilis* (Singh *et al*., 2010) and *Nostoc* spp. (Gao and Garcia-Pichel, 2011a), but has not been investigated in eukaryotic organisms.

Southern Ocean Sea Ice Algal Community

At its seasonal maximum extent (i.e. July), the sea ice that surrounds Antarctica covers an area (~ 20 million km^2) that is 50% larger than the continent and about 40% of the Southern Ocean (Lizotte, 2001). As the sea ice begins to retreat and the photoperiod increases in the austral spring, conditions are ripe for large phytoplankton blooms. Upwelling of nutrient-rich upper circumpolar deep water (UCDW) at the Antarctic Polar Front makes the Southern Ocean a very productive ecosystem (Ito *et al*., 2005). The community structure of sea ice algae is often influenced by physical processes, especially stratification of the water column and the mixed layer depth (MLD), as this impacts light and nutrient availability. In well-mixed water columns, with MLDs of 25-50 m, the sea

ice algal community is dominated by the prymnesiophyte, *Phaeocystis antarctica*, while the diatom, *Fragilariopsis cylindrus* is the dominant species in highly stratified waters (MLDs of 5-20 m) of the Ross Sea (Arrigo *et al.*, 1999). Diatoms typically make up over 90% of the phytoplankton community near ice floes and areas of meltwater (Kropuenske *et al.*, 2009; Petrou *et al.*, 2011), with *F. cylindrus* accounting for about 35% of the total diatom abundance (Kang and Fryxell, 1992).

Research Goals

The goal of this study was to investigate the impact of UVB exposure on *F. cylindrus* under various light and temperature conditions, representative of environmental changes due to increased Southern Ocean stratification. A control treatment, representative of the current Southern Ocean, was mimicked by low temperature and light (LTLL) experimental conditions. To understand how *F. cylindrus* might respond to UVR in an environment that has undergone an increase in ocean stratification, *F. cylindrus* was exposed to relatively high temperature and high light (HTHL) conditions. Two additional experiments were conducted to investigate the impact of UVR on *F. cylindrus* under elevated temperature only (HTLL) and elevated light only (LTHL) conditions. This experimental matrix allowed for a comparison to be made between an increase in both temperature and light and an increase in only one environmental variable (temperature or light) in order to determine which environmental condition was driving any observed response.

Each experiment utilized three UVB treatments: a control, a low UVB treatment corresponding to closed ozone hole conditions, and a high UVB treatment corresponding to open ozone hole conditions. Growth and photosynthetic parameters, as well as

9

photoprotective strategies, were measured to detect UVB-induced damage and repair

mechanisms. Exposure to UVB was expected to cause oxidative stress and photodamage

in *F. cylindrus* cultures, which would then activate photoprotective mechanisms. Under

the current climate conditions (LTLL), the impact of UVB was hypothesized to be

minimal, as neither elevated temperature nor elevated light level is present. Conversely,

the degree of photodamage and activation of photoprotective strategies was predicted to

be greatest under the future climate condition (HTHL), due to the added stresses of

elevated temperature and light level. Exposure to only one elevated environmental

variable (HTLL and LTHL experiments) was expected to result in UVB-induced damage

and photoprotection to a greater extent than under the current conditions (LTLL), but not

as great as under the future stratification conditions (HTHL). The ability of *F. cylindrus*

to activate photoprotective mechanisms following UVB exposure would provide this

species with a competitive advantage as the Southern Ocean becomes more stratified due

to climate change.

Materials and Methods

Experimental Conditions

Four experiments were conducted, each utilizing either a 'high' (4°C) or 'low' (0°C) temperature and either a 'high' (100 µE m^{-2} s^{-1}) or 'low' (15 µE m^{-2} s^{-1}) continuous light level. Cultures of *F. cylindrus* (CCMP 1102) were grown semi-continuously in nutrient replete L1+Si growth medium under the experimental conditions for at least five generation times (about 2-4 weeks) prior to the experiment. Three days before the start of the experiment, the batch culture was diluted (to an initial cell density of about 700,000 cells/mL) and divided into 18-2L bottles, with 6 replicates per UVB treatment. Within each experiment, cultures were exposed to one of three treatments: a control of 0% UVB:total irradiance, a low UVB treatment of 0.1% UVB:total irradiance, and a high UVB treatment of 2% UVB:total irradiance (Table 1). Low UVB cultures were placed into acid-washed polycarbonate bottles, while the high UVB cultures were placed into acid-washed Teflon bottles, which are transparent to UV radiation. The control cultures were kept in both polycarbonate and Teflon bottles (3 per bottle type) to control for any effects due to bottle material. Black plastic was used to cover the UV lamp for the control treatment bottles. A random number generator was used to assign bottle locations within the ethylene glycol bath solution, used to control temperature. (Figure 3) A Jaz Spectrometer (Ocean Optics, Inc., Dunedin, FL) was used to measure UVB (290-320 nm) and PAR (400-750 nm) irradiance levels within the bottles. Each experiment was carried out for 96 hours, with most samples being collected at time 0 (prior to UVR exposure), 12, 24, 48, 72 and 96 hours thereafter. Samples to be analyzed on the flow cytometer (cell cycle analysis and cell viability) were not collected at the 12-hour time point. Cell density

measurements were taken at 0, 24 and 96 hours. Cultures were diluted following the 24-hour time point by replacing the volume (750 mL, dilution factor of 1.375) removed from sample collection with fresh medium.

The UVB irradiances used for the high and low UVB treatments are comparable to the irradiances measured by Moreau *et al*. (2014) near Tierra del Fuego. In the Moreau study, UVB-exposure experiments were conducted using natural solar radiation, as well as enhanced UVB radiation. Their 'natural' control conditions are similar to the low UVB treatment in the present study, as it was representative of UVB irradiances when the Antarctic ozone hole is closed. The natural UVB irradiance measured at a depth of 10% light penetration was 0.8 ± 0.4 μW cm^{-2} (0.008 ± 0.004 W m^{-2}), while the low UVB treatment in our experiment had a UVB irradiance level of 0.004 W m^{-2} under high light and 0.001 W m^{-2} under low light (Table 1). The elevated UVB irradiance used by Moreau *et al*. was equivalent to a 60% loss in the ozone layer (similar to the high UVB treatment in the present study), and was measured as 5 ± 0.8 μW cm^{-2} (0.05 ± 0.008 W m^{-2}) at a depth of 10% light penetration (Moreau *et al*., 2014). At the high light level, the high UVB irradiance was 0.07 W m^{-2} and was 0.02 W m^{-2} at the low light level (Table 1).

Growth and Photosynthesis

Cell density and biovolume were determined using a Coulter Counter (Beckman Multisizer™ 3 Coulter Counter®, Brea, CA). Sample aliquots of 500 µL were diluted in 20 mL of filtered seawater. Abundance and volume data were obtained for cells measuring between 2 and 8 µm in diameter. Culture samples for cell cycle analysis were preserved with 20 µL 25% glutaraldehyde per 1 mL of sample. Samples were stored at -80ºC until processed. Prior to analysis, samples were thawed, 10 µL of SYBR Green I

were added and samples were incubated at 80°C in the dark for 10 min. Analyses were performed on a sorting flow cytometer (MoFlo® Astios™, Beckman Coulter, Brea CA), equipped with a 488 nm laser. DNA-per-cell frequency distribution histograms were constructed using SYBR Green I fluorescence (513$\pm$26 nm) as the x-axis. The data were imported into ModFit LT 4.1 (Verity Software House), where a simple, diploid model was used to integrate under and between peaks corresponding to G1 and G2 phases. Statistical analysis was conducted on the percentage of cells in each phase independently of the percentage of cells in the other two phases.

Photosynthetic efficiency of photosystem II (Fv/Fm) and cross-sectional area of photosystem II were measured using a fast repetition rate fluorometer (FRRF; Fast Tracka® Chelsea, Inc., West Mosely, Surrey, U.K.). Samples were dark adapted for 30 minutes at 0°C prior to analysis and during analysis the flow cell was packed with ice to maintain a low temperature. *In vivo* and extracted chlorophyll *a* concentrations were measured using a fluorometer (10-AU™ Turner Designs, Sunnyvale, CA). To determine extracted chlorophyll *a* concentrations, 25 mL of sample were filtered onto GF/F (Whatman) filters and extracted in 5 mL of 90% acetone for 24 hours at -20°C prior to analysis.

Cell viability was measured on the flow cytometer (MoFlo® Astios™, Beckman Coulter, Brea CA) using SYTOX green. The SYTOX stain penetrates compromised cell membranes and stains the DNA, which allows it to be used to assess loss of membrane integrity and necrotic cell death. To each 1mL sample, 1μL of 50μM SYTOX was added. A vehicle control (1μL DMSO) was used to set a cutoff point for the classification of 'unhealthy' (i.e. leaky cell membranes) viewed as positively-stained cells. All samples

were incubated in the dark for 20 minutes. Fluorescence on the flow cytometer was measured at 520 nm.

HPLC Pigment Analysis

Sample aliquots of 75 mL were filtered onto GF/F (Whatman) filters, which were wrapped in foil and stored at -80ºC until processing. For analysis, pigments were extracted overnight in 1390 µL 100% HPLC grade acetone and 10 µL trans-β-Apo-8'-carotenal (internal standard). Approximately 24 hours later, 600 µL of extract were filtered (0.2 µm syringe-filter) and run on an Agilent 1100 Series HPLC (Agilent Technologies, Santa Clara, CA). This HPLC method utilizes a Waters Symmetry C8 column (4.6x150 mm, 3.5 µm packing size), with binary mobile phases (methanol:acetonitrile:0.25 M pyridine (50:25:25 v:v:v) and methanol:acetonitrile:acetone (20:60:20 v:v:v (DiTullio and Geesey, 2002)). Chromatograms were analyzed with Chemstation software (Rev B.04.03; Agilent Technologies).

Mycosporine-like Amino Acid Identification and Quantification

Particulate absorption spectra were collected using the Shimadzu UV-1601 spectrophotometer (Shimadzu Corporation, Kyoto, Japan) and analyzed using UV Probe (version 1.11) software. Twenty-five mL of sample were filtered onto GF/F (Whatman) filters. A reference filter blank of filtered seawater was subtracted from sample spectra. Action spectra were collected from 275-750 nm. From the resulting spectra, the absorbance at 334 nm (absorbance maximum for several MAAs) and 675 nm (chlorophyll *a* absorbance maximum) were recorded, allowing for the ratio of Abs_{334}/Abs_{675} to be calculated.

Statistical Analysis

Prior to statistical analysis, outliers from each set of six replicates were removed using the Grubbs outlier test (Grubbs, 1969), resulting in only 5 replicates (N=5) being used in the statistical analysis of each experiment. Mixed effect models were then used to determine the impact of UVB treatment on each measured variable, within each of the four experiments. For each model, treatment and sampling time (hour) were considered fixed effects, while sample replicate (1-18; 6 per treatment) was considered as a random effect. This allowed for the repeated sampling from the 18 cultures over the course of the experiment to be accounted for. ANOVAs were then carried out between the model and a null model, in which treatment had been removed, to determine the significance of treatment on the measured variable ($p<0.05$). If the models detected a significant impact of treatment, a series of Mann-Whitney-Wilcoxon tests was run to determine between which treatments, and at which time points, the significant differences occurred. Because this involved a second set of statistical analyses, a Bonferroni correction was used, such that the resultant p-values from the tests were compared to a critical alpha-value of 0.025 (0.05/2) (Weisstein). Linear models (response variable as a function of time) were used to detect any changes in the measured responses of the UVB treatments over the 96 hours of the experiment.

A second set of mixed effect models were used to test for significant differences between the four experiments. In these models, sampling time and experiment (LTLL, HTLL, LTHL, and HTHL) were the fixed effects with sample replicate remaining a random effect. ANOVAs between the model and null model (with experiment removed), were able to detect significant differences between the experiments. Tukey's post-hoc

tests were used to determine between which experiments the significant differences occurred ($p < 0.05$).

In order to better understand the impact of high levels of UVB on the measured response variables between the four experiments, the high UVB data from each experiment were normalized to the respective control treatment data. This resulted in the high UVB values being reported as a percent of the control data, with the control values normalized as 100%. Any time the high UVB data are lower than 100%, the original high UVB treatment data for that measured response were lower than the control treatment. Likewise, when the normalized high UVB data are higher than 100%, the original high UVB data for that measured response were higher than the control data. These data are shown in several of the following figures.

Results

Growth and Photosynthesis

Cell densities (cells mL^{-1}) of the control and low UVB *F. cylindrus* cultures were not significantly different in the LTLL, HTLL and LTHL experiments (ANOVA, p>0.05). However, under the HTHL experimental conditions, both the low and high UVB treatments had significantly greater cell densities than the control cultures after 24 hours of UVB exposure, yet by 96 hours, the low UVB and control were not significantly different, and the high UVB cell density was lower than the control (Figure 4; Mann-Whitney-Wilcoxon, p<0.025). There was a significant increase in cell density in the control cultures over the 96 hours of all four experiments, as well as in the low UVB treatments of the HTLL and LTHL experiments. There was no change with time in the low UVB treatment of the LTLL and HTHL experiments (linear model, p=0.54 and 0.08, respectively). By 96 hours, in all but the HTLL experiment, the high UVB-treated cultures had significantly lower cell densities than the control cultures (Figure 5). When linear models were fit to the high UVB cell densities for each of the four experiments, the HTLL conditions resulted in an increase (p=3.5x10^{-4}, slope=3.3x10^{3}) in cell density, while the LTHL conditions produced a decrease (p=6.3x10^{-3}, slope=-2.8x10^{-3}) in cell density (Figure 4). The linear models fit to the LTLL and HTHL showed no change in cell density (p>0.05) during the course of the experiments.

Because cell density measurements were taken at 0, 24 and 96 hours after initial UVB exposure, growth rates were calculated between 0 and 24 hours, 24 and 96 hours, and 0 and 96 hours (μ= ln N$_t$ – ln N$_0$ / t). Across all three UVB treatments, the 0-24 hour growth rates in both of the low light experiments were negative (Figure 6A). Under the LTHL experimental conditions, the high UVB treatment had a negative 0-24 hour growth

rate, while that of the control and low UVB treatments were positive and were similar to pre-experiment growth rates (0.3 day^{-1}) (Figure 7A). The highest growth rates during the first 24 hours following UVB exposure were found under the HTHL conditions. Here, growth rates were 2-3 times higher than pre-experiment growth rates. In both of the low light experiments, the growth rates between 24 and 96 hours increased relative to the first 24 hours, such that positive growth rates were observed (Figure 6B). The high UVB cultures had significantly lower growth rates under the LTLL conditions (Mann-Whitney-Wilcoxon, p<0.025). A similar decrease in high UVB 24-96 hour growth rate was also seen in the LTHL experiment, yet with a negative growth rate in this treatment. Conversely, under the HTHL conditions, the high UVB treatment had significantly higher growth rates than the control cultures (Figure 7B). The growth rates for the entire duration of the experiments (0 to 96 hours), showed significantly lower growth in the high UVB treatments with respect to the control cultures, while there was no significant differences between the low UVB and control treatments (Figure 6C, Mann-Whitney-Wilcoxon, p<0.025). The high UVB growth rates under the low temperature conditions, regardless of light level, were negative over the 96 hours of these two experiments (Figure 7C). Across all three UVB treatments, the LTLL experimental conditions resulted in the lowest growth rates.

The exposure to high UVB significantly impacted the percentage of cells in each phase of the cell cycle. Under all environmental conditions, only a very small percentage of cells (0-5%) were in the G2/M phase by 96 hours (Figure 8). Prior to entering G2/M, the cells must have completed DNA replication, which occurs in the S phase. Because the percentage of cells in the G2/M phase was so low, DNA replication was either not

occurring, or not occurring successfully, which resulted in an accumulation of cells in S phase without making the transition to the G2/M phase. Under the LTHL conditions, the cultures exposed to high UVB did not appear to be cycling through the phases, as the percent of cells in each of the phases was the same at 0, 24 and 96 hours (Figure 8). Yet, under the same experimental conditions, the control and low UVB treatment cultures appeared to be transitioning through the cell cycle.

Photosynthetic efficiency of PSII (as Fv/Fm) in *F. cylindrus* cultures exposed to low UVB levels was not significantly different from the control cultures in any of the experiments (Figure 9, Mann-Whitney-Wilcoxon, $p<0.025$). Changes in Fv/Fm in the control and low UVB cultures were minimal across the 96 hours of each experiment, as the data fit linear regression models with slopes ranging from 2.8×10^{-5} to 8.5×10^{-4} ($p<0.05$). Across all four experiments, high UVB resulted in significant decreases in the photosynthetic efficiency following 12 hours of exposure when compared to the control cultures (except in the HTLL experiment, where this decrease became significant after 48 hours of exposure) (Figure 9). There was no difference between the high UVB data from the LTLL and HTHL experiments (Tukey's post-hoc, $p>0.05$). Both high light experiments had lower Fv/Fm values than the low light conditions, with roughly 90% decreases in photosynthetic efficiency in LTHL and HTHL and only 50-70% decreases in LTLL and HTLL. At each light level, the increase in temperature resulted in higher photosynthetic efficiencies, when compared to the low temperature data (Tukey's post-hoc, $p<0.05$). The LTHL conditions facilitated the greatest high UVB-induced decrease in Fv/Fm, as the photosynthetic efficiency for the last 24 hours of the experiment was only 5% of the respective control (Figure 10).

The cross-sectional area of photosystem II was not significantly different in

control and low UVB-exposed *F. cylindrus* cells across all four experiments (Mann-

Whitney-Wilcoxon, $p > 0.025$). However, there was a significant difference in PSII area in

the control and low UVB cultures between the low and high light conditions. Based upon

the intercepts from the linear models, cells acclimated to the low light level had larger

PSII at 720-750 nm^2 $quanta^{-1}$, while the high light acclimated cultures had reduced cross-

sectional areas of approximately 650 nm^2 $quanta^{-1}$ ($p < 0.05$) (Figure 11). In the LTLL

experiment, the high UVB treatment resulted in significantly larger PSII, starting at 12

hours. Similar increases in PSII size were seen in the high UVB cultures in both high

temperature experiments (HTLL and HTHL) at 96 hours (Mann-Whitney-Wilcoxon,

$p < 0.025$). Under the LTHL experimental conditions, a significant increase in PSII cross-

section was present at 48 hours following high UVB exposure. After this time, the size of

PSII becomes highly variable and appears to decrease, yet is not significantly different

than the data from the control cultures. No significant differences were observed between

the cross-sectional area of PSII among the four experiments (Tukey's post-hoc, $p > 0.05$)

(Figure 12).

Chlorophyll *a* concentrations in the low UVB *F. cylindrus* cultures were rarely

significantly different from the control cultures. In both the control and low UVB

cultures, chlorophyll *a* concentrations increased over the 96 hours of each experiment

(slopes were positive and significantly different than zero) (Figure 13). *F. cylindrus*

cultures exposed to high UVB had significantly lower concentrations of chlorophyll *a*

than the control cultures, after the initial 48 hours of the experiment (after the initial 24

hours in the HTHL experiment) (Mann-Whitney-Wilcoxon, $p < 0.025$). There was no

significant difference observed in the impact of high UVB exposure across the four

experiments (ANOVA, p>0.05) (Figure 14). No differences in the chlorophyll *a* per cell

concentrations between the control and low UVB treatments were detected during any of

the experiments (Figure 15). Lower chlorophyll *a* per cell concentrations were found in

cells exposed to high UVB compared to cells exposed to no UVB in all experiments

except LTLL (Mann-Whitney-Wilcoxon, p<0.025). This decrease became significant

after the initial 24 hours in the HTHL experiment, but was not significant in the HTLL

and LTHL experiments until 96 hours. However, the high UVB treatments across all four

experiments were not significantly different (ANOVA, p>0.05) (Figure 16).

The cell viability data are reported here as the percent of total cells that are

'healthy' (i.e. intact cell membrane), based upon the amount of fluorescence produced by

the SYTOX stain. In all four experiments, the low UVB-treated cultures were not

significantly different from the control cultures (Mann-Whitney-Wilcoxon, p>0.025).

There was no change in the percent of healthy cells in the control cultures in either of the

low light experiments (LTLL and HTLL) over the duration of the experiments. Under the

high light conditions, there was a slight increase (linear model, p=4.7×10^{-4}, slope =0.1) in

the percent of healthy cells at low temperature (LTHL) and a slight decrease (p=3.5×10^{-4},

slope=-0.0003) in the percent of healthy cells at the high temperature (HTHL) conditions

(Figure 17). In the low UVB-treated cultures, there was no significant change in the

proportion of healthy cells over the 96 hours in either of the high temperature

experimental conditions. In both of the low temperature experiments, there was a small

(both slopes of 0.06), but significant increase in the percent of healthy cells in the

cultures exposed to low UVB. The percent of healthy cells was significantly lower in the

high UVB treatment in the LTLL and LTHL experiments, starting at 24 and 48 hours after UVB exposure, respectively (Mann-Whitney-Wilcoxon, p<0.025) (Figure 17). However, the impact of high UVB on *F. cylindrus* cultures in the high temperature experiments was not the same as under the low temperatures conditions. In the HTLL experiment, the high UVB treated cells were only significantly different at 72 hours. Under the HTHL conditions, the high UVB cultures had significantly lower proportions of healthy cells at 24 and 48 hours. Yet following the 48-hour time point, the percent of healthy cells in the high UVB cultures continued to decrease, but this also occurred in the control cultures, making the high UVB treatment not significantly different from the control (Figure 17). There was no significant difference of the percent healthy cells between any of the four experiments (Tukey's post-hoc, p>0.05) (Figure 18).

Xanthophyll Cycle and Pigment Analysis

Changes in the ratio of photoprotective:photosynthetic (Pp:Ps) pigments under the various environmental conditions provided insight into the importance of pigment functions. In the LTLL, HTLL and HTHL experiments, this pigment ratio in the low UVB-exposed cultures was not significantly different than the control cultures (Figure 19). However, in the LTHL experiment, the low UVB treatment had a significantly higher Pp:Ps ratio than the control for the last 24 hours of the experiment (Mann-Whitney-Wilcoxon, p<0.025). Results of the linear regression analysis showed that over the duration of each experiment, there was either no change or a decrease in photoprotective pigments in the control and low UVB cultures. In *F. cylindrus* exposed to high UVB, significant increases in photoprotective pigments were detected after 48 hours

(after 24 hours in HTHL), while there were no differences between the high UVB data of the four experiments (Tukey's post-hoc, p>0.05) (Figure 20).

Evidence of xanthophyll cycling was detected by an increase in the ratio of diatoxanthin (DT) concentration to total diadinoxanthin and diatoxanthin (DD+DT) concentration (as DT:(DD+DT)). There was no significant evidence to support xanthophyll cycling in the *F. cylindrus* cultures exposed to the low UVB treatment, when compared to the control cultures. Under all experimental conditions except HTHL, there was no change in DT:(DD+DT) over the 96 hours in the control or low UVB treatment (linear model, p>0.05) (Figure 21). The linear models fit to the control and low UVB data from the HTHL showed slopes significantly different than zero (p=5×10^{-4} and 8×10^{-6}, respectively), yet these were very small (slope=3×10^{-5} and 6×10^{-4}, respectively). Significant increases in DT:(DD+DT) were observed between the high UVB treatment and the respective control in all experiments except LTLL (Mann-Whitney-Wilcoxon), where there was also no change over the course of the experiment (linear model, p=0.93). Xanthophyll cycling activity was lower under both high temperature experiments (HTLL and HTHL) than in the LTHL experiment (Figure 22). At the elevated temperature, significant evidence of the xanthophyll cycle was obtained for the last 24 hours at low light and for the last 48 hours at high light. Xanthophyll cycling in the high UVB-exposed cultures under the LTHL conditions was significantly higher than under the other three experimental conditions (Tukey's post-hoc, p<0.025) (Figure 22). In this experiment, a significant increase in DT:(DD+DT) of the high UVB treatment was present following the first 24 hours of UVB exposure, and by 96 hours, DT:(DD+DT) was 3.5 times greater than the control.

Not only is xanthophyll cycling driven by the conversion between diadinoxanthin and diatoxanthin, but its physiological significance is also a function of the total pool of these pigments. There was no significant difference in the xanthophyll pigment pool size between the control and low UVB treatments in the LTLL, HTLL or HTHL experiments (Figure 23). Under the LTHL experimental conditions, the low UVB treatment had a significantly larger xanthophyll pool than the control for the last 24 hours of the experiment (Mann-Whitney-Wilcoxon, $p < 0.025$). Across all experimental conditions, when the control and low UVB data were fit to linear models, the slopes were slightly, but significantly negative, suggesting a decrease in the xanthophyll pigment pool in these treatments during the 96 hours of the experiment. Significantly larger xanthophyll pools were found in *F. cylindrus* cultures exposed to high UVB under all temperature and light conditions, following 48 hours of exposure (after 24 hours in HTHL) (Figure 24). However, there was no significant change in the high UVB-exposed xanthophyll pool over the course of the experiments (linear model, $p > 0.05$). However, there was no significant difference in the xanthophyll pigment pool between the four experiments (Tukey's post-hoc, $p > 0.05$).

Mycosporine-like Amino Acids

The presence of MAAs was preliminarily detected by measuring the absorbance at 334 nm (MAA absorbance maximum) relative to the absorbance at 675 nm (chlorophyll *a* absorbance maximum). The MAA content in *F. cylindrus* cultures of the low UVB treatment was rarely significantly different than the control cultures, and when this did occur (only in the low light experiments), the low UVB cultures had lower MAA content than the control cultures (Mann-Whitney-Wilcoxon, $p < 0.025$) (Figure 25). There

was no significant change in MAA content in the control and low UVB cultures throughout the duration of any of the four experiments (linear model, p>0.05). Each of the four experiments had at least one time point at which the MAA content of the high UVB treatment was significantly greater than the control. This occurred for the last 24 hours in the LTLL experiment and at the last time point (96 hours) in the HTLL experiment. Under both of the high light experimental conditions, the MAA content of the high UVB-exposed cultures was greater than the control cultures for the final 48 hours (Figure 25). The MAA content in the high UVB treatment was the greatest under the LTHL experimental conditions, being almost 3 times greater than the control, and about twice as great as under the HTHL conditions (having the second greatest MAA content) (Figure 26). This resulted in the high UVB treatment of the LTHL experiment being significantly different than the other three experiments, with no difference between those three (LTLL, HTLL and HTHL) (Tukey's post-hoc, p>0.05).

Discussion

Overall, the results of this study showed that high UVB exposure (i.e. "open" ozone hole levels of UVB) significantly impaired the growth and photosynthetic competency of the diatom *F. cylindrus*, and resulted in increased activation of photoprotective mechanisms. In contrast, low level UVB exposure (i.e. levels similar to a "closed" Southern Ocean ozone hole) did not significantly impact the physiological performance of *F. cylindrus*, compared to cultures exposed to no UVB. Physiological responses to high UVB exposure were dependent upon the temperature and light conditions to which the cells were acclimated. For instance, growth and photosynthetic parameters were preferentially impacted by high UVB levels in the LTHL experiment, while *F. cylindrus* was the least impacted by high UVB under the LTLL conditions. There was relatively little, if any, induction of photoprotective mechanisms in the LTLL treatment, while xanthophyll cycling and elevated production of photoprotective pigments and MAAs were all observed in the LTHL experiment relative to the control.

Prior to conducting the four experiments in this study, it was hypothesized that high UVB-induced damage and stimulation of photoprotective mechanisms would be minimal under the current Southern Ocean environmental conditions of low temperature and low light. It was also predicted that *F. cylindrus* under the future ocean stratification conditions of high temperature and high light would be the most damaged by UVB, resulting in the greatest activation of photoprotective mechanisms. The current ocean stratification hypothesis was supported by the data, but the hypothesis describing future ocean stratification conditions was not substantiated. Surprisingly, high UVB exposure most significantly affected *F. cylindrus* under elevated light conditions only (i.e. LTHL).

F. cylindrus grown under elevated temperature only, also exhibited decreased growth and photosynthesis and increased activation of photoprotective mechanisms, but to an intermediate degree, as hypothesized, compared to the LTLL and LTHL experiments.

At both light levels, elevated temperature ameliorated the negative impact of high UVB exposure relative to cultures grown at 0°C. For instance, the HTLL and HTHL treatments resulted in smaller decreases in growth and photosynthesis and smaller increases in the activation of photoprotective mechanisms than the respective low temperature experiments (Figures 7, 10, 22 and 26). Regardless of light level, the increase in temperature partially mitigated the detrimental effects of high UVB exposure on photosynthetic efficiency and growth rate (0-96 hour at LL and 0-24 and 24-96 hour at HL) (Figures 7 and 10). At the high light level, *F. cylindrus* grown at the high temperature had significantly lower xanthophyll cycling and MAA content than at the low temperature. These results were unexpected, as the added stressor of elevated temperature was hypothesized to exacerbate the detrimental effects of high UVB exposure. The mitigating role of elevated temperature relative to other concomitant stressors appears to be a taxonomically diverse response. For example, a study conducted by Cabrerizo *et al*. (2014), exposed four temperate phytoplankton species (*Alexandrium tamarense*, *Chaetoceros gracilis*, *Dunaliella salina*, and *Isochrysis galbana*) to UV radiation (42.8 W m^{-2} UVA and 0.7 W m^{-2} UVB) at three different temperatures (14, 17 and 20°C), to which the cultures had been pre-acclimated. UV radiation decreased photosynthetic rates (as μmol O$_2$ μg Chl a^{-1} h^{-1} and quantum yield of PSII) and increased PSII inhibition in all four species. At the higher temperatures, *A. tamarense* (a dinoflagellate) and *D. salina* (a chlorophyte) showed a continued decrease in

photosynthesis and increase in photoinhibition. In contrast, however, as the temperature

increased, *C. gracilis* (a diatom) and *I. galbana* (a haptophyte) showed increased

photosynthetic rates and decreased photoinhibition relative to the lower temperature

cultures (Cabrerizo *et al*., 2014). These latter temperature results were similar to those

observed herein for *F. cylindrus* exposed to high UVB under relatively high temperature

(Figures 10, 22 and 26).

This same temperature trend was also found by other investigators in Antarctic

phytoplankton species. For example, Roos and Vincent (1998) exposed *Phormidium*

murrayi, an Antarctic cyanobacterium, to UVA (125 μW cm^{-2} or 1.25 W m^{-2}) and UVB

(25 μW cm^{-2} or 0.25 W m^{-2}) radiation along with increasing temperatures (5ºC, 10 ºC, 15

ºC and 20ºC). The growth rates of *P. murrayi* over the 5-day experiment were lower

following UV exposure, yet increased with increasing temperature. In the present study,

F. cylindrus growth rates were also significantly lower in UVB-exposed cultures over the

96 hours (4 days) of each experiment, with higher growth rates measured at the higher

temperature. Maximum photosynthetic rates of *P. murrayi* were not significantly

impacted by UV radiation, but increased roughly 3-fold with increasing temperature.

Phormidium murrayi had reduced cellular chlorophyll *a* concentrations (as μg (mg dry

weight)$^{-1}$) when exposed to both UVA and UVB radiation at a range of PAR levels of

10-500 μE m^{-2} s^{-1}, with the greatest reduction occurring at the higher light levels (>60 μE

m^{-2} s^{-1}) (Roos and Vincent, 1998). A similar decrease in chlorophyll *a* per cell was

detected in the present study following exposure to UVB; however, this reduction was

not significantly impacted by light intensity (no significant difference between 15 and

100 μE m^{-2} s^{-1}) (Figure 16). The ratio of photoprotective carotenoids to chlorophyll *a*

(similar to the ratio of photoprotective to photosynthetic pigments in the present study) was significantly higher in *P. murrayi* exposed to UV radiation, regardless of light intensity, yet this ratio was the least affected by UV radiation at the higher temperature (20ºC compared to 10 and 15ºC) (Roos and Vincent, 1998). Similarly, *F. cylindrus* cultures exposed to high levels of UVB had higher ratios of photoprotective to photosynthetic pigments (as also observed in *P. murrayi*); however, there was no significant impact of temperature or light level.

Reduced photosynthetic competency (e.g. growth rate, Fv/Fm) and elevated photoprotective mechanisms (e.g. xanthophyll cycling, MAAs) in the LTHL treatment, in combination with elevated photosynthetic performance and a lowered photoprotective response in the HTLL relative to the control LTLL condition demonstrates the delicate intracellular physiological balance that occurs whenever multiple stressors are involved. For instance, elevated temperature will increase enzymatic photochemical reactions that will enhance photosynthetic efficiency of PSII and result in elevated growth rates. At supersaturating light levels (i.e. irradiances higher than I_k) excess energy cannot be effectively dissipated by photosynthesis and photoprotective pathways, thereby resulting in decreased growth rates. This effect is exacerbated under low temperature conditions where photochemistry is not maximal due to suppressed enzymatic activity.

For several of the measured responses (photosynthetic efficiency, photoprotective pigments, xanthophyll cycling and MAA content), high UVB exposure had a significant impact starting at 24 or 48 hours. Prior to this point in the experiment, *F. cylindrus* cultures exposed to high levels of UVB were statistically the same as those cultures exposed to no UVB. As many of these physiological responses can be altered over the

course of minutes to hours (Brunet *et al.*, 2011; Motokawa *et al.*, 2014) it is interesting that these changes were often not detected until at least a day after initial UVB exposure. This result suggests that short-term mechanisms (e.g. ROS scavenging by antioxidants) may alleviate oxidative stress temporarily. In addition, several studies have shown that UVB-induced physiological responses are dose-dependent, such that organisms may be able to tolerate UVB-exposure until a threshold level of radiation has been absorbed (Neale *et al.*, 1998; Behrenfeld *et al.*, 1993; Smith *et al.*, 1980). Since *F. cylindrus* does not appear to be immediately affected by high levels of UVB, the amount of UVB radiation may not reach a threshold until 24-48 hours. But this temporal lag on the threshold level is no doubt dependent on the prior light history, as well as the magnitude of the radiation dose.

The synthesis of photoprotective carotenoids is often employed as a protective mechanism following exposure to high light stress. However, the role of carotenoids as a UVB-inducible photoprotective strategy remains controversial (Cockell and Knowland, 1999). The increased abundance of carotenoids, including xanthophyll cycle pigments, has been shown to be stimulated by UVB exposure in species of cyanobacteria (Ehling-Schulz *et al.*, 1997; Götz, *et al.*, 1999), diatoms (Laurion and Roy, 2009) and natural phytoplankton communities (Smith *et al.*, 1992). Because most carotenoids have absorbance maxima in the visible and not ultraviolet range of wavelengths, this form of photoprotection is most likely based upon the ability of carotenoids to quench ROS, and not to prevent absorption of UVB by the cell (Gao and Garcia-Pichel, 2011b; Cockell and Knowland, 1999). In the research presented here, *F. cylindrus* exposed to high levels of UVB had significantly higher relative concentrations of photoprotective pigments and

greater activation of xanthophyll cycling, compared to the control cultures (Figures 19 and 21). Yet this response may be driven by elevated oxidative stress as a result of UVB exposure, rather than a direct response to the UVB radiation itself. Regardless of the specific function of these carotenoids when it comes to photoprotection, their induction by UVB may provide *F. cylindrus* with a competitive advantage over other more susceptible species (e.g. *Phaeocystis antarctica* (Arrigo *et al*., 2010; Kropuenske *et al*., 2009)) in a highly stratified Southern Ocean.

Evidence of xanthophyll cycling was detected by an increase in the ratio of diatoxanthin (DT) concentration to total diadinoxanthin and diatoxanthin (DD+DT) concentration. As a photoprotective mechanism, xanthophyll cycling is expected to be active following exposure to high light, and in this case, exposure to high UVB as well. An increase in this ratio was observed in the high UVB treated cultures under all environmental conditions, except LTLL. It is likely that these current ocean stratification conditions do not provide a great enough light stress to induce xanthophyll cycling, even under high UVB exposure. However, under the same light conditions, but at elevated temperature, xanthophyll cycling was active during the last 24 hours of the HTLL experiment, suggesting that temperature alone may be able to impact xanthophyll cycle activity, perhaps via temperature enhancement of de-epoxidase activity. This was also detected at the high light level, yet the impact of temperature appeared to be the opposite. Here, xanthophyll cycling was not as active under the elevated temperature as it was under the low temperature condition. At first glance, this response could be due to the cells requiring greater photoprotection under the low temperature conditions. However, it is also possible that this is a result of the cells not being able to successfully convert

diadinoxanthin to diatoxanthin at this elevated temperature. This conversion is carried out by the de-epoxidase enzyme, which is activated by a decrease in pH as a result of a proton gradient across the thylakoid membrane. Yet, in order for this to occur, the cellular and chloroplast membranes need to be functional. Analysis of the STYOX cell viability data from the present study can shed some light on the condition of *F. cylindrus* cell membranes following UVB exposure. In the HTHL experiment, where there was a decrease in xanthophyll cycle activity (compared to the LTHL experiment), there were also significant decreases in the percent of healthy cells in both the control and high UVB cultures during the 96 hours of the experiment, which was significantly lower than the other three experiments. This suggests that the HTHL conditions, with and without the addition of UVB exposure, caused membrane damage. The accumulation of UV-induced ROS has been shown to induce the lipid oxidation of cellular membranes (Murphy, 1983), which can be especially damaging to chloroplast membranes because of the strong photooxidative potential of this organelle (Malanga, 1997). Poppe *et al*., (2003) found UVB (0.60-0.85 W m $^{-2}$) resulted in the deformation and ultimately disintegration of thylakoid membranes of four red algal species (*Palmaria decipeins*, *Palmaria palmate*, *Phycodrys austrogeorgica*, *Bangia atropurpurea*) after only 2 hours of exposure. Based upon these results, Poppe *et al*. (2003), hypothesized that maintenance of the proton gradient across a UVB-damaged thylakoid membrane would very difficult. If, in the present study, the SYTOX data are indicative of thylakoid, as well as cellular, membrane damage, this could suggest that the reduced xanthophyll cycle activity in the HTHL experiment, was a result of the cells' inability to convert diadinoxanthin to diatoxanthin, and possibly not due to a lesser need for this photoprotective mechanism. However,

because the growth and photosynthesis data showed less UVB-induced damage, the original hypothesis of reduced xanthophyll cycling because of a reduced need for photoprotection remains valid.

In the present study, MAAs assessed by spectrophotometric measurements were only detected under the high light conditions, when *F. cylindrus* cultures were exposed to high levels of UVB radiation. Since relatively low concentrations of MAAs (estimated by Abs_{334}/Abs_{675}) were detected under the low light conditions, it can be hypothesized that exposure to this lower UVB irradiance was not sufficient to stimulate MAA synthesis in *F. cylindrus*. UVB-induction of MAA production is consistent with several other studies of Antarctic phytoplankton. For example, when exposed to UVB+PAR, four diatoms (*Thalassiosira* sp., *Corethron criophilum*, *Pseudo-nitzschia* sp., and *F. cylindrus*) responded by synthesizing MAAs (Helbling *et al*., 1996). In the two centric species (*Thalassiosira* sp. and *Corethron criophilum*), there was significant MAA production under natural PAR (no UVR) as well, while UVB radiation was required to induce the synthesis of MAAs in the pennate species (*Pseudo-nitzschia* sp., and *F. cylindrus*). These findings are also consistent with those in the present study, since relatively low amounts of MAAs, if any, were detected in the control or low UVB treatments. Of the over twenty currently described MAAs, *F. cylindrus* has been shown to be able to produce shinorine, porphyra-334 and mycosporine-glycine:valine (Gröniger *et al*., 2000; Helbling *et al*., 1996; Riegger and Robinson, 1997). However, mass spectrometric analysis is needed to determine the presence of other MAAs present in lower concentrations. The present study was able to detect the presence of MAAs in *F. cylindrus* cultures; however, the identification and quantification of these compounds will require detailed analytical methods in order to be

verified. These data are anticipated to provide more substantial evidence of MAA production and yield insight into the MAA synthesis pathway in *F. cylindrus*.

Under all experimental conditions, exposure to high UVB caused photosynthetic damage (Figure 9). However, this did not always result in the induction of xanthophyll cycling or MAA production as photoprotective mechanisms (Figures 17 and 23). This begs the question, "Are other means of photoprotection actively involved instead?" Because UVB causes oxidative stress (Dubey and Prasad, 2014), increasing the concentration of cellular antioxidants could be a protective strategy. It is conceivable that *F. cylindrus* might be responding to high UVB exposure by producing other antioxidants, as enzymes or metabolites, rather than simply activating xanthophyll cycling or MAA synthesis. There are several enzymes that function as antioxidants, including superoxide dismutase, ascorbate peroxidase, catalase and glutathione reductase, among others (Table 2). The activity of these enzymes will be determined in a planned RNA gene-expression analysis employing material from experiments conducted in the present study. MAAs and carotenoids (β-carotene) have been shown to have antioxidant properties (Oren and Gunde-Cimerman, 2007), as do other cellular compounds such as DMSP and its degradation products (Sunda *et al*., 2002), ascorbic acid and glutathione (Roy, 2000). Analysis of these compounds was not included herein, but may provide information on the oxidative stress level of these cells.

Another mechanism that could be activated by UVB-induced photodamage involves repair of photosystem II via the D1 protein. UV radiation has been shown to directly damage PSII, as well as produce reactive oxygen, which can also damage PSII (Lesser, 1996). In this repair mechanism, the D1 protein of the photodamaged PSII

(induced by UV or blue light) is digested. A pre-D1 protein is synthesized and inserted into the PSII. The pre-D1 protein is processed to form the finalized D1 protein and the PSII is re-assembled and becomes functional (Takahashi and Murata, 2008). The rate of D1 protein repair is affected by temperature and light intensity, with repair being inhibited by low temperature and high light (Takahashi and Murata, 2008). These are the environmental conditions under which the high UVB-exposed *F. cylindrus* cultures displayed the highest photosynthetic impairment and employed the greatest degree of xanthophyll cycling and MAA production. Since these stressful conditions inhibit D1 repair, it is reasonable to suggest that *F. cylindrus* resorted to other photoprotective mechanisms, like xanthophyll cycling and MAA production, to overcome the photosynthetic damage caused by high UVB exposure. Hence, it is hypothesized that the reduction in photosynthetic parameters under the LTHL conditions may be due to the inability to repair D1 protein damage inflicted by high UVB exposure. In this regard, future RNA gene expression analysis will provide important information to test this D1protein damage hypothesis.

While the irradiances used in the current research are comparable to those measured by Moreau *et al*. (2014), those measurements were made at light depths equivalent to 10% incident irradiance, which in the open ocean is often observed at around 30 m (Kirk, 1994). Bracher and Wiencke (2000) measured UVB irradiance levels at a depth of 5 m within the Antarctic Polar Front, where the maximum UVB levels were 0.33 to 0.62 W m^{-2}. In their study, incubation experiments were conducted using low (0.2 to 0.3 W m^{-2}) and high (0.5 to 0.7 W m^{-2}) UVB treatments, representative of normal and depleted ozone concentrations, respectively (Bracher and Wiencke, 2000). The UVB

level of Bracher and Wiencke's low UVB treatment was about 100x greater than the low UVB treatment used in the present study and their high UVB treatment was about 10x greater than that of the present study. Ryan *et al*. (2012) measured surface UVB irradiances with maximum values of about 1.3 W m^{-2}. Based upon these results, experiments were conducted on sea ice algae using UVB irradiances of 0.0157, 0.0785, 0.157, and 0.314 W m^{-2} (approximately 1%, 6%, 12% and 24% of surface UVB measurements). Significant decreases in photosynthesis were only detected at the two highest UVB irradiances (0.157 and 0.314 W m^{-2}) (Ryan *et al*., 2012). However, in the research presented here, UVB exposure had significant detrimental impacts on *F. cylindrus* photosynthesis at levels comparable to the two lowest UVB irradiances used in the Ryan et al. study. When compared to these two studies the UVB levels used herein may be a conservative estimate of UVB fluxes in surface waters of the Southern Ocean. This could mean that the response of *F. cylindrus* to UVB exposure observed in the present study may not be truly representative of how this species would respond in natural surface waters. If this is the case, it is expected that in the Southern Ocean, *F. cylindrus* would be exposed to higher levels of UVB, which would result in a greater extent of photoinhibition and likely a correspondingly greater activation of photoprotective mechanisms.

Interpretation of the results obtained in the present study should be done cautiously, with the understanding that the *F. cylindrus* cultures were acclimated to incident PAR and temperature for a minimum of 5 generation times before the experiments started. Incubation and mesocosm experiments in the field typically do not pre-acclimate natural populations to various environmental conditions. Hence results

from the current lab experiments may not reflect true physiological changes occurring in natural populations after an abrupt change in ambient conditions (e.g. change in the vertical mixing rate). Similarly, adaptation responses in nature over long timescales (e.g. decades) may lead to different physiological responses than those measured here due to short-term acclimation changes as well as long-term changes in genetic selection. It should also be noted that a single, lab-raised isolate of *F. cylindrus* was used in this series of experiments, which may not accurately represent the diversity of this species or it's response to natural UVB in the Southern Ocean.

Roos and Vincent (1998) summarized their findings by stating that the cellular response to an environmental stressor depends upon the balance between damage caused by that stressor and the cell's ability to prevent or repair that damage. In the present study, the response of *F. cylindrus* to UVB exposure is a balance between oxidative stress (i.e. ROS production) resulting in photodamage and the activation of photoprotective mechanisms (i.e. photoprotective pigments and MAAs). This physiological balance will favor inhibition if there is an increase in photodamage (increased UVB irradiance or inhibition of repair mechanisms) or a decrease in photoprotection (inhibited biosynthesis by environmental factors). Herein, *F. cylindrus* grown at the elevated light level and low temperature was more susceptible to photodamage and triggered photoprotective mechanisms when exposed to high levels of UVB, indicating that increased irradiance shifts the physiological response to UVB towards photoinhibition. Conversely, at the elevated temperature, exposure to the high UVB treatment resulted in less photodamage and lower photoprotection activity, which suggests that the increase in temperature is able to shift the balance towards protection and repair, presumably by allowing

biochemical carbon fixation to act as an energy overflow mechanism. This could be due to cellular enzymatic processes occurring faster at warmer temperatures, which may allow protective and repair mechanisms to be more active.

However, it is important to note that climate change in the Southern Ocean will not only result in changes in temperature and light due to an increase in ocean stratification. *F. cylindrus* and the Southern Ocean phytoplankton community will also be subject to increases in ocean acidification and decreases in pH and nutrient/trace metal availability (especially iron), which may further complicate the balancing act involved in tolerating UVB radiation. Only by understanding this complex matrix of environmental stressors can we attempt to predict the physiological response of the phytoplankton community to elevated UVB levels, as a result of stratospheric ozone depletion.

Overall, the present findings lead to the conclusions that *F. cylindrus* is negatively affected by UVB under conditions representative of an open Antarctic ozone hole. However, the degree of this negative impact and the photoprotective response will depend upon the future temperature and light conditions of the Southern Ocean. Under current climate conditions, *F. cylindrus* underwent significant photodamage, yet the measured photoprotective mechanisms were not activated. An elevated light level appeared to cause the greatest amount of damage and both the xanthophyll cycle and MAA production were highly active. Unexpectedly, the future climate conditions, and elevated temperature in general, appeared to provide *F. cylindrus* a UVB mitigation strategy, which will likely be highly advantageous with the future warming of the Southern Ocean.

Works Cited

Arrigo, K.R., Robinson, D.H., Worthen, D.L., Dunbar, R.B., DiTullio, G.R., VanWoert, M. & Lizotte, M.P. (1999). Phytoplankton community structure and the drawdown of nutrients and CO_2 in the Southern Ocean. *Science, 283*, 365-367.

Arrigo, K.R., Mills, M.M., Kropuenske, L.R., van Dijken, G.L., Alderkamp, A.C. & Robinson, D.H. (2010). Photophysiology in two major Southern Ocean phytoplankton taxa: Photosynthesis and growth of *Phaeocystis Antarctica* and *Fragilariopsis cylindrus* under different irradiance levels. *Integrative and Comparative Biology, 50* (6): 950-966.

Behrenfeld, M.J., Chapman, J.W., Hardy, J.T. & Lee II, H. (1993). Is there a common response to ultraviolet-B radiation by marine phytoplankton? *Marine Ecology Progress Series, 102*, 59-68.

Bettwy, M. (2003). A season in the life of the Antarctic Ozone Hole: a quarter century of satellite measurements by TOMS. [Internet]. Retrieved from http://www.nasa.gov/vision/earth/lookingatearth/25TOMSAGU.html

Bracher, A.U. and Wiencke, C. (2000). Simulation of the effects of naturally enhanced UV radiation on photosynthesis of Antarctic phytoplankton. *Marine Ecology Progress Series, 196*, 127-141.

Brunet, C., Johnsen, G., Lavaud, J. & Roy, S. (2011). Pigments and photoacclimation processes. In S. Roy, C.A. Llewellyn, E.S. Egeland & G. Johnsen (Eds.), *Phytoplankton pigments* (445-471). Cambridge, England: Cambridge University Press.

Cabrerizo, M.J., Carrillo, P., Villafañe, V.E. and Helbling, E.W. (2014). Current and predicted global change impacts of UVR, temperature and nutrient inputs on photosynthesis and respiration of key marine phytoplankton groups. Journal of Experimental Marine Biology and Ecology. 461:371-380.

Callone, A. I., Carignan, M., Montoya, N. G., & Carreto, J. I. (2006). Biotransformation of mycosporine like amino acids (MAAs) in the toxic dinoflagellate Alexandrium tamarense. *Journal of photochemistry and photobiology. B, Biology*, *84*(3), 204–12.

Capotondi, A., Alexander, M.A., Bond, N.A., Curchitser, E.N., and Scott, J.D. (2012). Enhanced upper ocean stratification with climate change in the CMIP3 models. J. Geophys. Res., 117,C04031.

Carreto, J.I., & Carignan, M.O. (2011). Mycosporine-like amino acids: relevant secondary metabolites, chemical and ecological aspects. *Marine Drugs, 9*, 387-446.

Cockell, C.S. & Knowland, J. (1999). Ultraviolet radiation screening compounds. *Biological Reviews, 74*, 311-345.

Díaz, S.B., Morrow, J.H., & Booth, C.R. (2000). UV physics and optics. In S. de Mora, S. Demers & M. Vernet (Eds.), *The effects of UV radiation in the marine environment* (pp. 35-71). Cambridge, England: Cambridge University Press.

DiTullio, G. & Geesey, M.E. (2003). Photosynthetic pigments in marine algae and bacteria. *Encyclopedia of Environmental Microbiology*.

Dubey, G. & Prasad, S.M. (2014). Differential display of antioxidants in mitigating adverse effects of UV-B radiation in *Nostoc muscorum* and *Phormidium foveolarum* photoacclimated to different irradiances. *Applied Biochemistry and Biotechnology*.

Ehling-Schulz, M., Bilger, W. & Scherer, S. (1997). UV-B induced synthesis of photoprotective pigments and extracellular polysaccharides in the terrestrial cyanobacterium *Nostoc commune*. *Journal of Bacteriology, 179*, 1940-1945.

Falkowski, P.G. & Raven, J.A. (1997). *Aquatic photosynthesis*. Malden, MA: Blackwell Science.

Favre-Bonvin, J., Bernillon J., Salin, N., & Arpin, N. (1987). Biosynthesis of mycosporines: mycosporine glutaminol in *Trichothecium roseum*. *Phytochemistry, 29*, 2509-2514.

Gao, Q. & Garcia-Pichel, F. (2011a). An ATP-grasp ligase involved in the last biosynthetic step of the iminomycosporine shinorine in *Nostoc punctiforme* ATCC 29133. *Journal of Bacteriology*.193(21):5923-5928.

Gao, Q. & Garcia-Pichel, F. (2011b). Microbial ultraviolet sunscreens. *Nature Reviews Microbiology, 9*, 791-802.

Götz, T., Windhovel, U., Böger, P & Sandmann G. (1999). Protection of photosynthesis against UV-B radiation by carotenoids in transformants of the cyanobacterium *Synechococcus* PCC 7942. *Plant Physiology, 120*, 599-604.

Gröniger, A., Sinha, R.P., Klisch, M. & Häder, D.-P. (2000). Photoprotective compounds in cyanobacteria, phytoplankton and macroalgae-a database. *Journal of Photochemistry and Photobiology B: Biology, 58*, 115-122.

Grubbs, F.E. (1969). Procedures for detecting outlying observations in samples. *Technometrics,11*(1):1-21.

Helbling, E.W., Chalker, B.E., Dunlap, W.C., Holm-Hansen, O. & Villafañe, V.E. (1996). Photoacclimation of Antarctic marine diatoms to solar ultraviolet radiation. *Journal of Experimental Marine Biology and Ecology*, *204*, 85-101.

Huntley, M.E., Lopez, M.D. & Karl, D.M. (1991). Top predators in the Southern Ocean: a major leak in the biological pump. *Science, 253*, 64-66.

Ito, T., Parekh, P., Dutkiewicz, S. & Follows, M.J. (2005). The Antarctic circumpolar productivity belt. *Geophysical Research Letters, 32*(L13604).

Kang, S.H. & Fryxell, G.A. (1992). Fragilariopsis cylindrus (Grunow) Krieger: The most abundant diatom in water column assemblages of Antarctic marginal ice-edge zones. *Polar Biology, 12*(6-7), 609-627.

Karsten, U., Franklin, L.A., Lüning, K. & Wiencke, C. (1998). Natural ultraviolet radiation and photosynthetically active radiation induce formation of mycosporine-like amino acids in the marine macroalgae *Chondrus crispus* (Rhodophyta). *Planta, 205*, 257-262

Kirk, J.T.O. (1994). Optics of UV-b radiation in natural waters. Arch. Hydrobiol. Beih., 43, 1-16.

Kopczynska, E.E., Savoye, N., Dehairs, F., Cardinal, D. & Elskens, M. (2007). Spring phytoplankton assemblages in the Southern Ocean between Australia and Antarctica. *Polar Biology, 31*, 77-88.

Kropuenske, L.R., Mills, M.M., van Dijken, G.L., Bailey, S., Robinson, D.H., Welschmeyer, N.A. & Arrigio, K.R. (2010). Photophysiology in two major Southern Ocean phytoplankton taxa: Photoprotection in *Phaeocystis antarctica* and *Fragiliariopsis cylindrus*. *Limnology and Oceanography, 54*(4), 1176-1196.

Laurion, I. & Roy, S. (2009). Growht and photoprotection in three dinoflagellates (including two strains of *Alexandrium tamarense*) and one diatom exposed to four weeks of natural and enhanced ultraviolet-B radiation. *Journal of Phycology, 45*, 16-33.

Lesser, M.P. (1996). Elevated temperatures and ultraviolet radiation cause oxidative stress and inhibit photosynthesis in symbiotic dinoflagellates. *Limnology and Oceanography, 41*(2):271-283.

Lizotte, M.P. (2001). The contributions of sea ice algae to Antarctic marine primary production. *American Zoology, 41*, 57-73.

Malanga, G., Calmanovici, G. & Puntarulo, S. (1997). Oxidative damage to chloroplasts from *Chlorella vulgaris* exposed to ultraviolet-B radiation. *Physiologia Plantarum, 101*(3):455-462

Mewes, H. & Richter, M. (2002). Supplementary ultraviolet-B radiation induces a rapid reversal of the diadinoxanthin cycle in the strong light-exposed diatom *Phaeodactylum tricornutum. Plant Physiology 130*, 1527-1535.

Meyer, A.A., Tackx, M. & Daro, N. (2000). Xanthophyll cycling in *Phaeocystis globosa* and *Thalassiosira* sp.: a possible mechanism for species succession. *Journal of Sea Resreach, 43*(3-4), 373-384.

Moisan, T., Olaizola, M., & Mitchell, B.G. (1998). Xanthophyll cycling in Phaeocystis antarctica: changes in cellular fluorescence. *Marine Ecology Progress Series*, *169*, 113–121.

Moreau, S., Mostajir, B., Almandoz, G.O., Demers, S., Hernando, M., Lemarchand, L., Lionard, M., Mercier, B., Roy, S., Schloss, I.R., Thyssen, M. & Ferreyra, G.A. (2014). Effects of enhanced temperature and ultraviolet B radiation on a natural plankton community of the Beagle Channel (southern Argentina): a mesocosm study. *Aquatic Microbial Ecology, 72*:155-173.

Motokawa, S., Hattori, H., Sasaki, H. & Taguchi, S. (2014). Photoprotective acclimation of micro- and nano-size phytoplankton assemblages in the Indian sector of the Southern Ocean. *Polar Biology*.

Müller, P., Li, X., & Niyogi, K.K. (2001). Non-photochemical quenching: A response to excess light energy. *Plant Physiology, 125*, 1558-1566.

Murphy, T.M. (1983). Membranes as targets of ultraviolet radiation. *Physiologia Plantarum, 58*, 381-388.

Neale, P.J., Cullen, J.J. & Davis, R.F. (1998). Inhibition of marine photosynthesis by ultraviolet radiation: Variable sensitivity of phytoplankton in the Weddell-Scotia Confluence during the austral spring. *Limnology and Oceanography, 43*(3): 433-448.

Oren, A., & Gunde-Cimerman, N. (2007). Mycosporines and mycosporine-like amino acids: UV protectants or multipurpose secondary metabolites? *FEMS microbiology letters*, *269*(1), 1–10.

Petrou, K., Doblin, M.A. & Ralph, P.J. (2011). Heterogeneity in the photoprotective capacity of three Antarctic diatoms during short-term changes in salinity and temperature. *Marine Biology, 158*, 1029-1041.

Poppe, F., Schmidt, R.A.M., Hanelt, D. & Wiencke, C. (2003). pEffects of UV radiation on the ultrastructure of several red algae. *Phycological Research, 51*, 11-19.

Rastogi, R.P. & Incharoensakdi, A. (2013). UV radiation-induced accumulation of photoprotective compounds in the green alga *Tetraspora* sp. CU2551. *Plant Physiology and Biochemistry, 70*, 7-13.

Riegger, L. & Robinson, D. (1997). Photoinduction of UV-absorbing compounds in Antarctic diatoms and *Phaeocystis antarctica. Marine Ecology Progress Series, 160*, 13-25.

Roos, J.C. & Vincent, W.F. (1998). Temperature dependence of UV radiation on Antarctic cyanobacteria. *Journal of Phycology, 34*:118-125.

Rosic, N.N. (2012). Phylogenetic analysis of genes involved in mycosporine-like amino acid biosynthesis in symbiotic dinoflagellates. *Applied Microbiology and Biotechnology*.

Roy, S. (2000). Strategies for the minimisation of UV-induced damage. In S. de Mora, S. Demers & M. Vernet (Eds.), *The effects of UV radiation in the marine environment* (pp. 177-205). Cambridge, England: Cambridge University Press.

Ryan, K.G., McMinn, A., Hegseth, E.N. & Davy, S.K. (2012). The effects of ultraviolet-b radiation on Antarctic sea-ice algae. *Journal of Phycology, 48*, 74-84.

Sarmiento, J.L., Slater, R., Barber, R., Bopp, L., Doney, S.C., Hirst, A.C., Kleypas, J., Matear, R., Mikolajewicz, U., Monfray, P., Soldatov, V., Spall, S.A., & Stouffer, R. (2004) Response of ocean ecosystems to climate warming. *Global Biogeochemical Cycles, 18*, GB3003.

Singh, S.P., Klish, M., Sinha, R.P. & Häder, D.P. (2010). Genome mining of mycosporine-like amino acid (MAA) synthesizing and non-synthesizing cyanobacteria: A bioinformatics study. *Genomics, 95*, 120-128.

Sinha, R.P., Klisch, M., Helbling, E.W. & Häder, D.-P. (2001). Induction of mycosporine-like amino acids (MAAs) in cyanobacteria by solar ultraviolet-B radiation. *Journal of Photochemistry and Photobiology B: Biology, 60*(1-2), 129-135.

Shick, J.M., Romaine-Lioud, S., Ferrier-Pagès, C. & Gattuso, J.-P. (1999). Ultraviolet-B radiation stimulates shikimate pathway-dependent accumulation of mycosporine-like amino acids in the coral *Stylophora pistillata* despite decreases in its population of symbiotic dinoflagellates. *Limnology and Oceanography, 44*(7), 1667-1682.

Shick, J.M. & Dunlap, W.C. (2002). Mycosporine-like amino acids and related gadusols: biosynthesis, accumulation, and UV-protective functions in aquatic organisms. *Annual Review of Physiology, 64*, 223-262.

Smith, R.C., Baker, K.S.k, Holm-Hansen, O. & Olson, R. (1980). Photoinhibition of photosynthesis in natural waters. *Photochemistry and Photobiology, 31*, 585-592.

Smith, R.C., Prézelin, B.B., Baker, K.S., Bidigare, R.R., Boucher, N.P., Coley, T., Karentz, D., MacIntyre, S., Matlick, H.A., Menzies, D., Ondrusek, M., Wan, Z., & Waters, K.J. (1992). Ozone depletion: ultraviolet radiation and phytoplankton biology in Antarctic waters. *Science, 255*, 952-959.

Sobrino, C., Ward, M.L. & Neale, P.J. (2008). Acclimation to elevated carbon dioxide and ultraviolet radiation in the diatom *Thalassiosira pseudonana*: Effects on growth, photosynthesis and spectral sensitivity of photoinhibition. *Limnology and Oceanography, 53*, 494-505.

Speekmann, C.L., Bollens, S.M. and Avent, S.R. 2000. The effect of ultraviolet radiation on the vertical distribution and mortality of estuarine zooplankton. J. Plankton Res. 22(12): 2325-2350.

Sunda, W., Kieber, D.J., Kiene, R.P., & Huntsman, S. (2002). An antioxidant function for DMSP and DMS in marine algae. *Nature, 418:317-320*.

Takahashi, S. & Murata, N. (2008). How do environmental stresses accelerate photoinhibition? *Trends in Plant Science, 13*(4):178-182.

Vernet, M. (2000). Effects of UV radiation on the physiology and ecology of marine phytoplankton. In S. de Mora, S. Demers & M. Vernet (Eds.), *The effects of UV radiation in the marine environment* (pp. 237-278). Cambridge, England: Cambridge University Press.

Vernet, M., Brody, E.A., Holm-Hansen, O., & Mitchell, B.G. (1994). The response of Antarctic phytoplankton to ultraviolet radiation: absorption, photosynthesis, and taxonomic composition. In C.S. Weiler & P.A. Penhale (Eds), *Ultraviolet Radiation in Antarctica: Measurements and Biological Effects*, Antarctic Research Series (pp 143-158). Washington, DC: American Geophysical Union.

Vincent, W.F. & Neale, P.J. (2000). Mechanisms of UV damage to aquatic organisms. In S. de Mora, S. Demers & M. Vernet (Eds.), *The effects of UV radiation in the marine environment* (pp. 149-176). Cambridge, England: Cambridge University Press.

Weisstein, Eric W. "Bonferroni Correction." From *MathWorld*--A Wolfram Web Resource. http://mathworld.wolfram.com/BonferroniCorrection.html

Wood, W.F. (1989). Photoadaptive responses of the tropical red alga *Eucheuma striatum* Schmitz (Gigartinales) to ultra-violet radiation. *Aquatic Botany, 33*(1-2), 41-51.

Wu, Y., Campbell, D.A. & Gao, K., (2014). Faster recovery of a diatom from UV damage under ocean acidification. *Journal of Photochemistry and Photobiology B:Biology*.

Xu, K., Fu, F.X., & Hutchins, D.A. (2014). Comparative responses of two dominant Antarctic phytoplankton taxa to interactions between ocean acidification, warming, irradiance, and iron availability. *Limnology and Oceanography, 59(6)*:1919-1931.

Yamamoto, H. Y. (1985). [34] Xanthophyll cycles. *methods in Enzymology*,*110*, 303-312.

Zudaire, L. & Roy, S. (2001). Photoprotection and long-term acclimation to UV radiation in the marine diatom *Thalassiosira weissflogii. Journal of Photochemistry and Photobiology B: Biology, 62(1-2):*26-34.

Figures
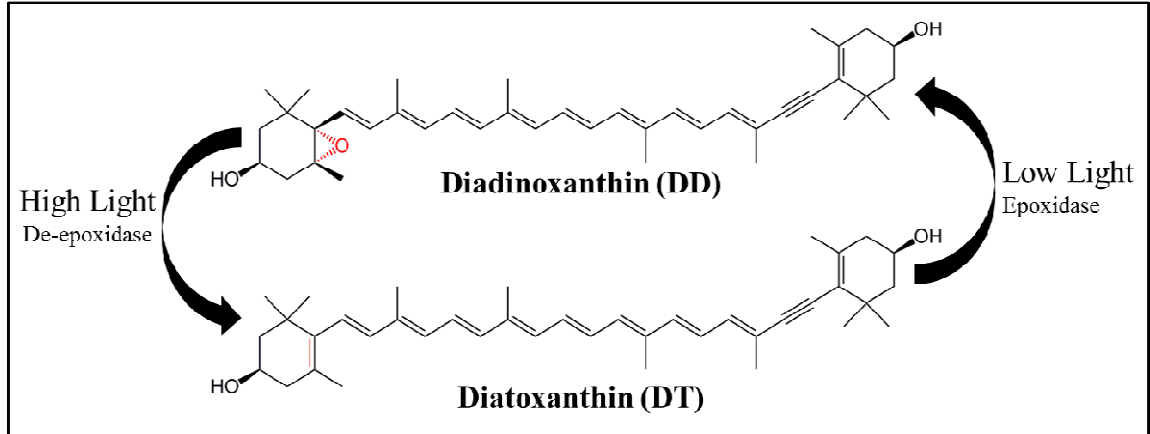
Figure 1. Xanthophyll cycling occurs via the conversion between diadinoxanthin and diatoxanthin by a de-epoxidase enzyme, which removes the epoxide from diadinoxanthin. High light conditions activate the formation of diatoxanthin from diadinoxanthin, while low light conditions activate the formation of diadinoxanthin from diatoxanthin.
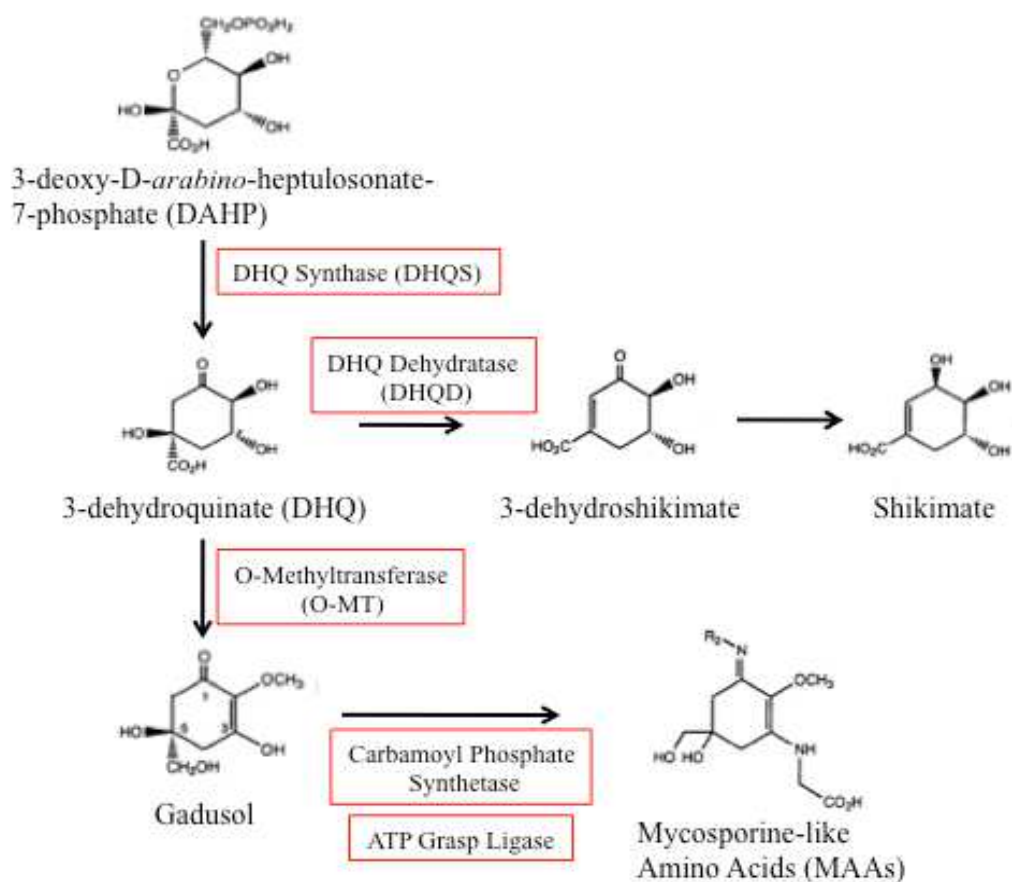
Figure 2. Synthesis of mycosporine-like amino acids occurs via the Shikimate pathway. Enzymes boxed in red are hypothesized to be involved in this synthesis pathway. Transcript expression levels for these genes will be determined by RNA-Seq analysis.
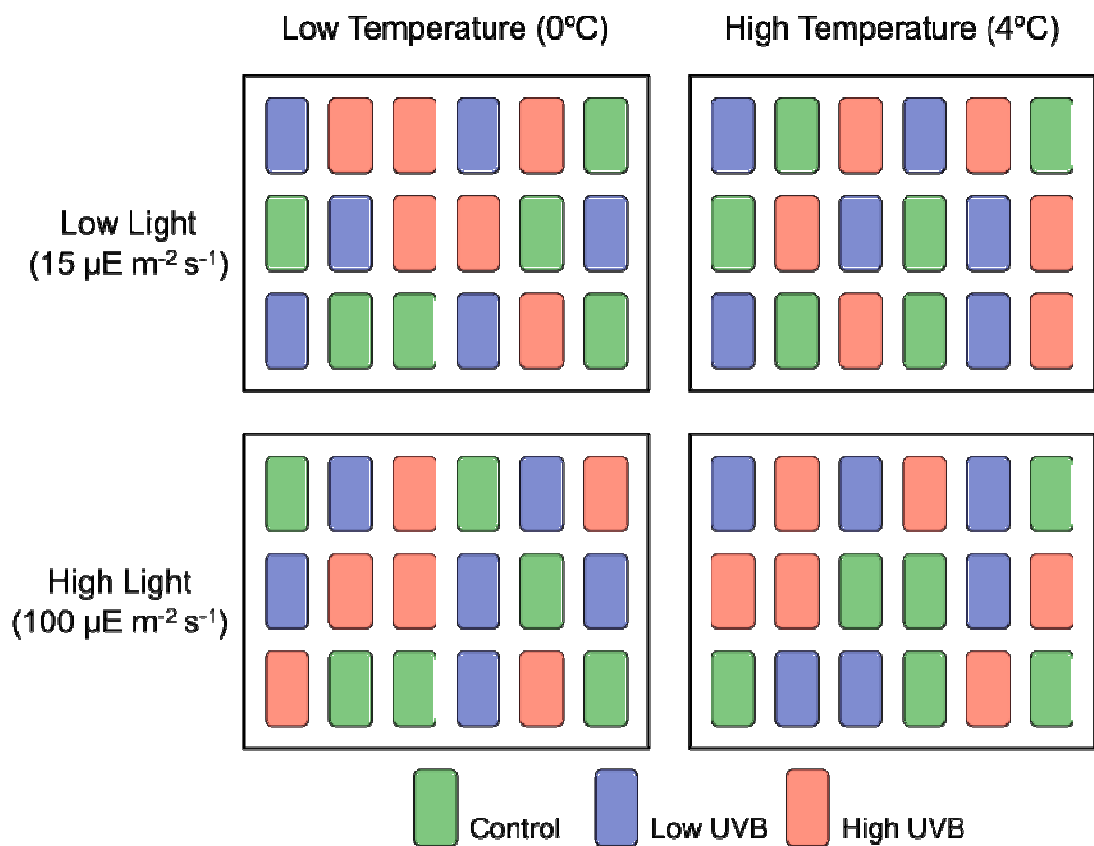
Figure 3. Schematic of temperature and light experiments and UV treatments within each experiment.
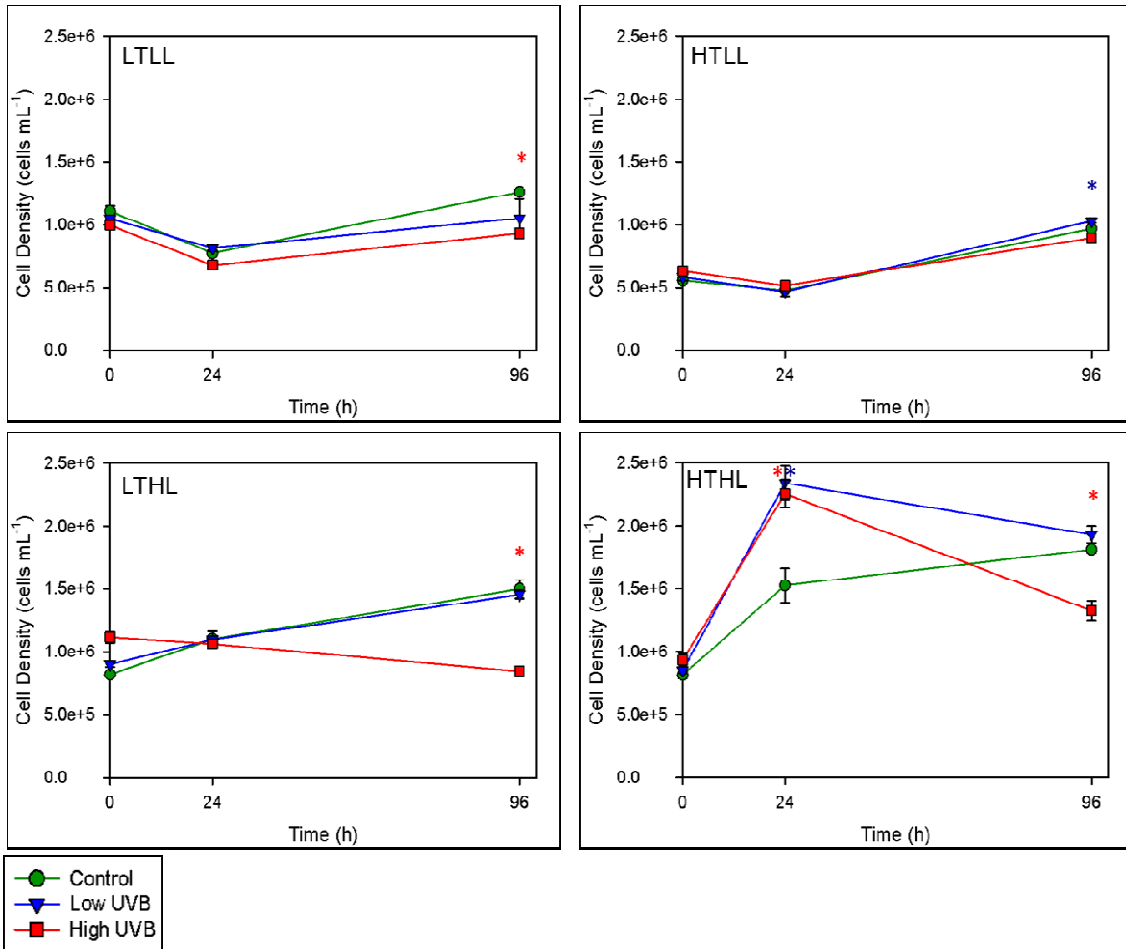
Figure 4. Mean cell densities (± standard error) for each of the four temperature and light experiments. Asterisks (*) represent significant differences (p<0.025) determined by Mann-Whitney-Wilcoxon tests between control and treatment represented by asterisk color.
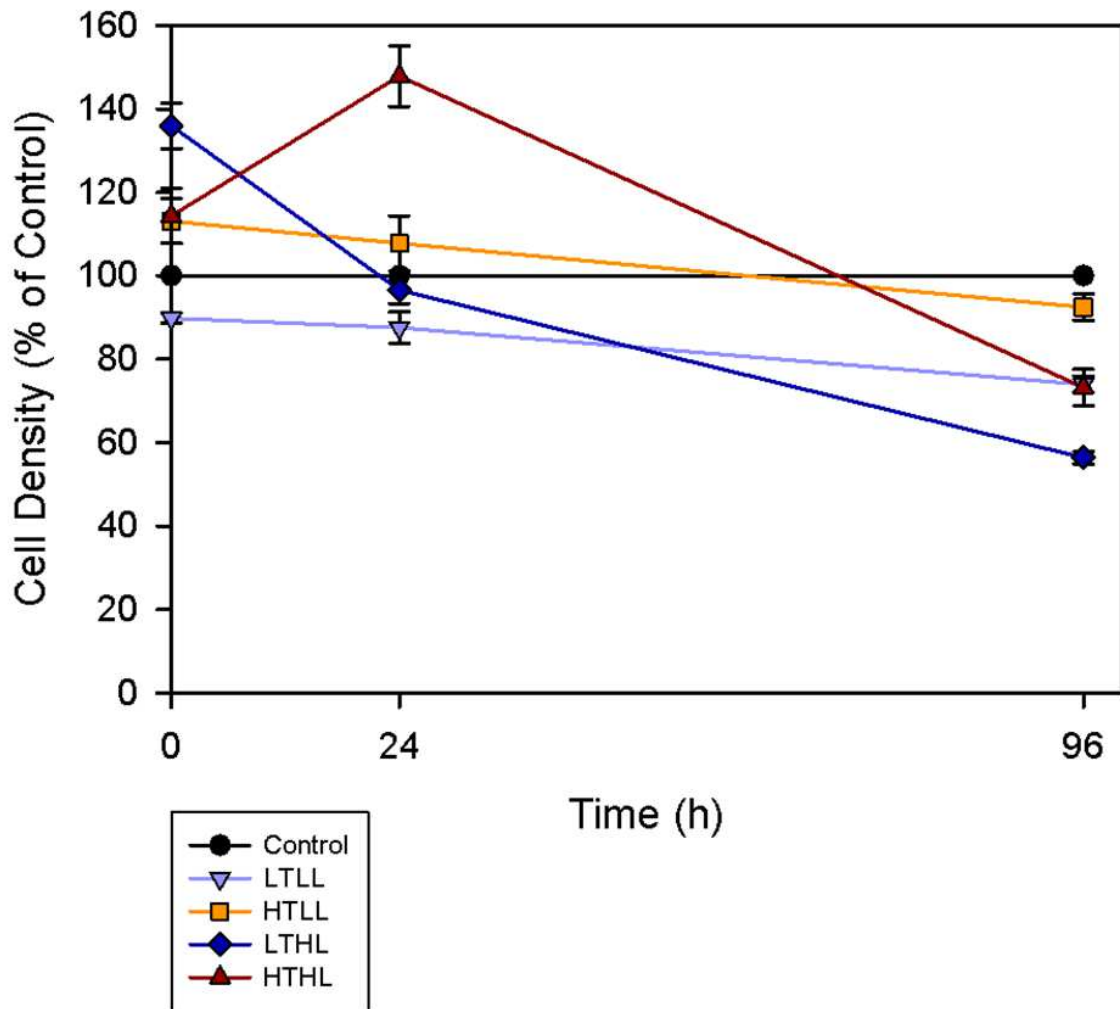
Figure 5. Mean cell densities ($\pm$ standard error) from each high UVB treatment normalized to the respective control treatment, shown as percent of the control treatment's cell density. The black line represents the control values, at 100%.
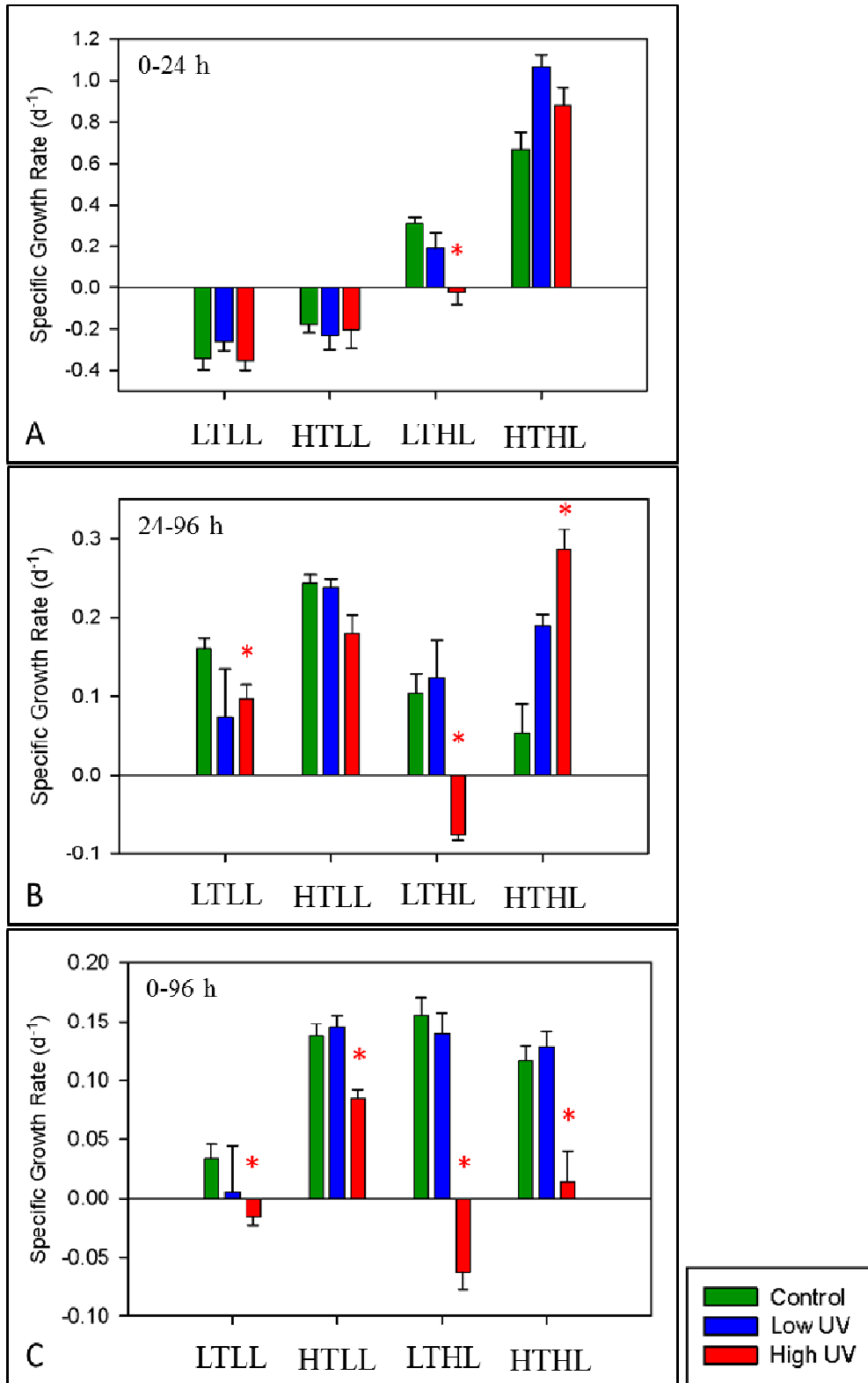
Figure 6. Mean specific growth rates (± standard error) (0-24 h, 24-96 h and 0-96 h) for each of the four light and temperature experiments. Asterisks (*) represent significant differences (p<0.025) determined by Mann-Whitney-Wilcoxon tests between control and treatment represented by asterisk color.
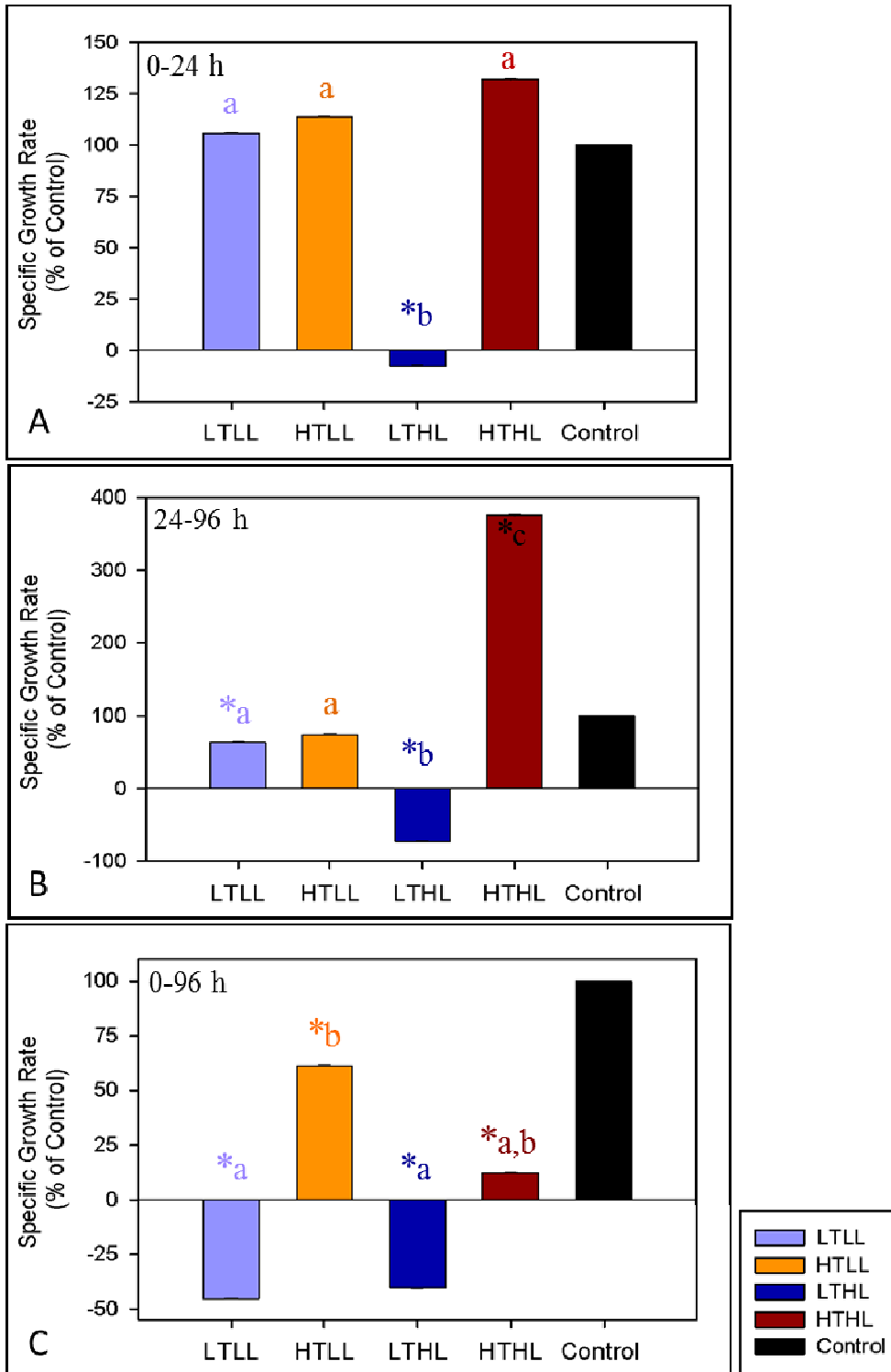
Figure 7. Mean specific growth rate (± standard error) (0-24 h, 24-96 h and 0-96 h) from each high UVB treatment normalized to the respective control treatment, shown as percent of the control treatment's specific growth rate. The black bar represents the control value, at 100%. Asterisks (*) represent a significant difference between the high UVB treatment and its respective control, as determined by Mann-Whitney-Wilcoxon tests. Letters (a, b, etc.) represent significant difference among experiments, as determined by Tukey's post-hoc analysis.
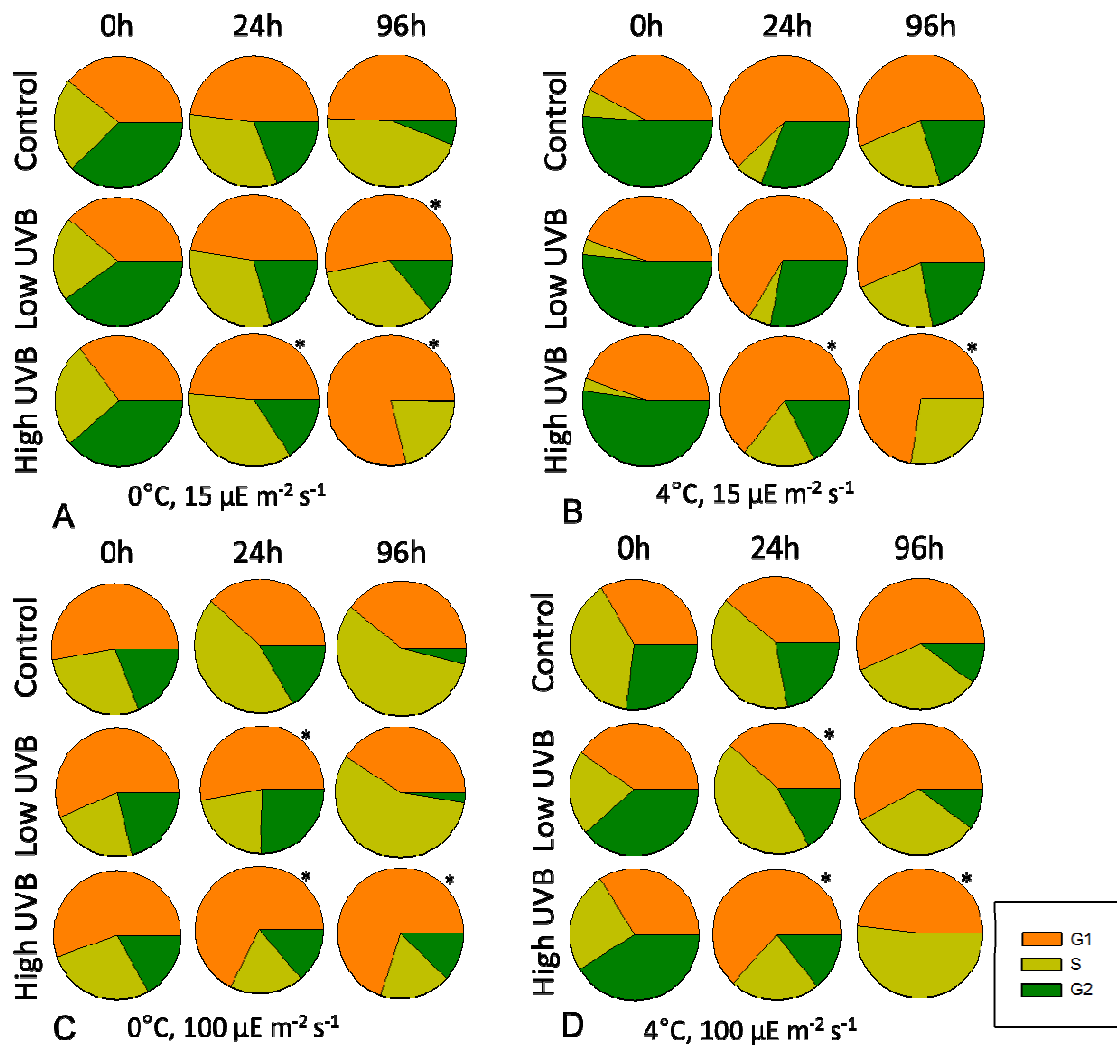
Figure 8. Mean percent of cells in G1, S or G2/M phases of the cell cycle for each of the four experiments. Asterisks represent significant difference (p<0.025) determined by Mann-Whitney-Wilcoxon tests between treatment and control.
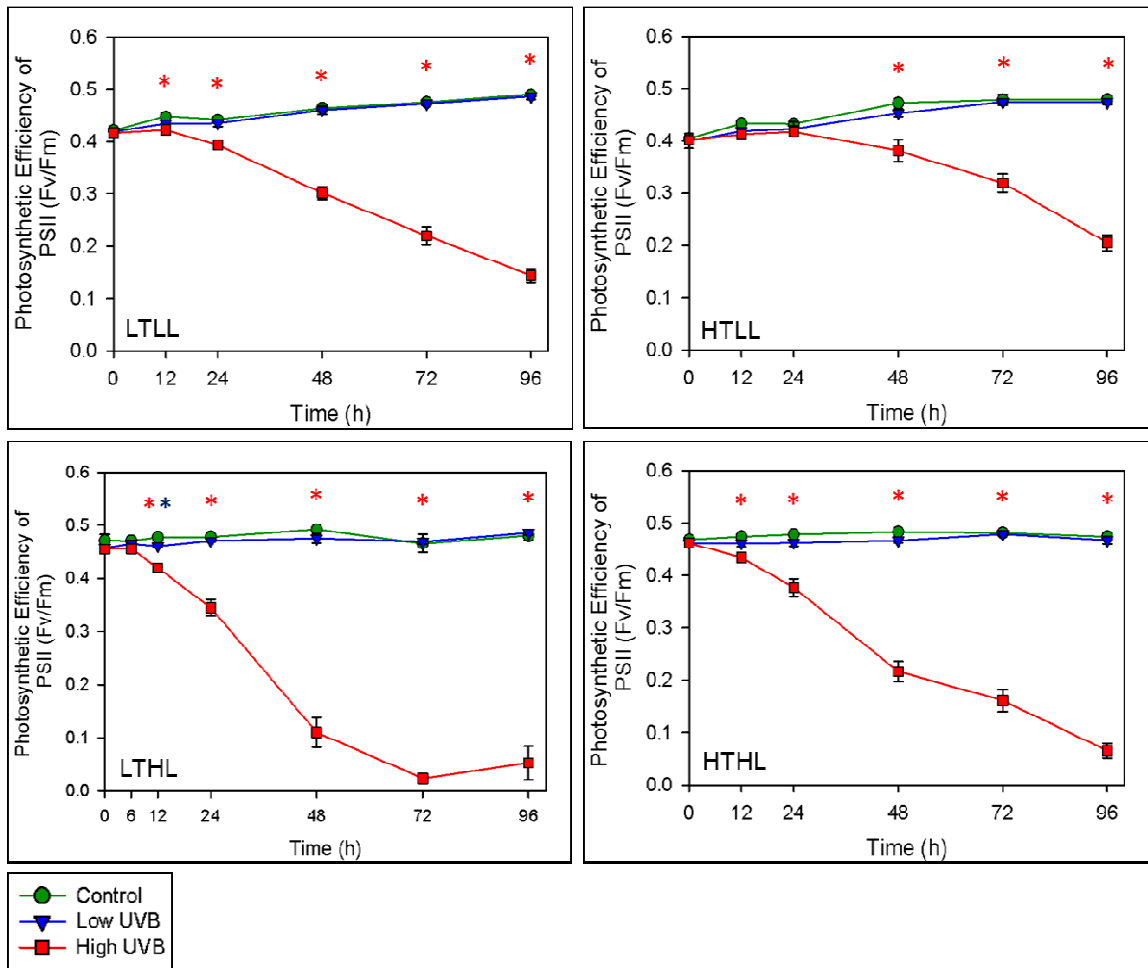
Figure 9. Mean photosynthetic efficiency of photosystem II (PSII) ($\pm$ standard error) for each of the four light and temperature experiments. Asterisks (*) represent significant differences (p<0.025) determined by Mann-Whitney-Wilcoxon tests between control and treatment represented by asterisk color.
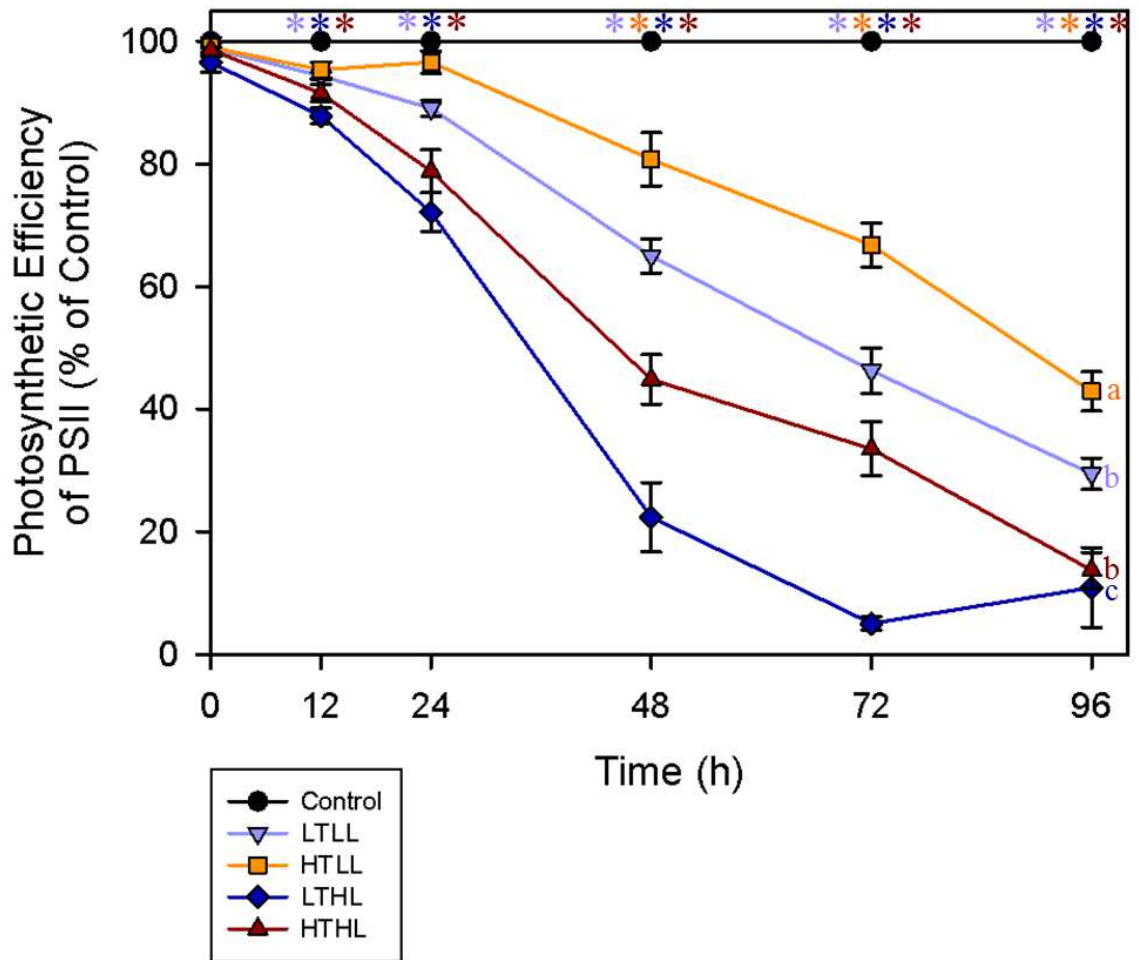
Figure 10. Mean photosynthetic efficiency of PSII ($\pm$ standard error) from each high UVB treatment normalized to the respective control treatment, shown as percent of the control treatment's Fv/Fm value. The black line represents the control value, at 100%. Asterisks (*) represent a significant difference between the high UVB treatment and its respective control, as determined by Mann-Whitney-Wilcoxon tests. Letters (a, b, etc.) represent significant difference among experiments, as determined by Tukey's post-hoc analysis.
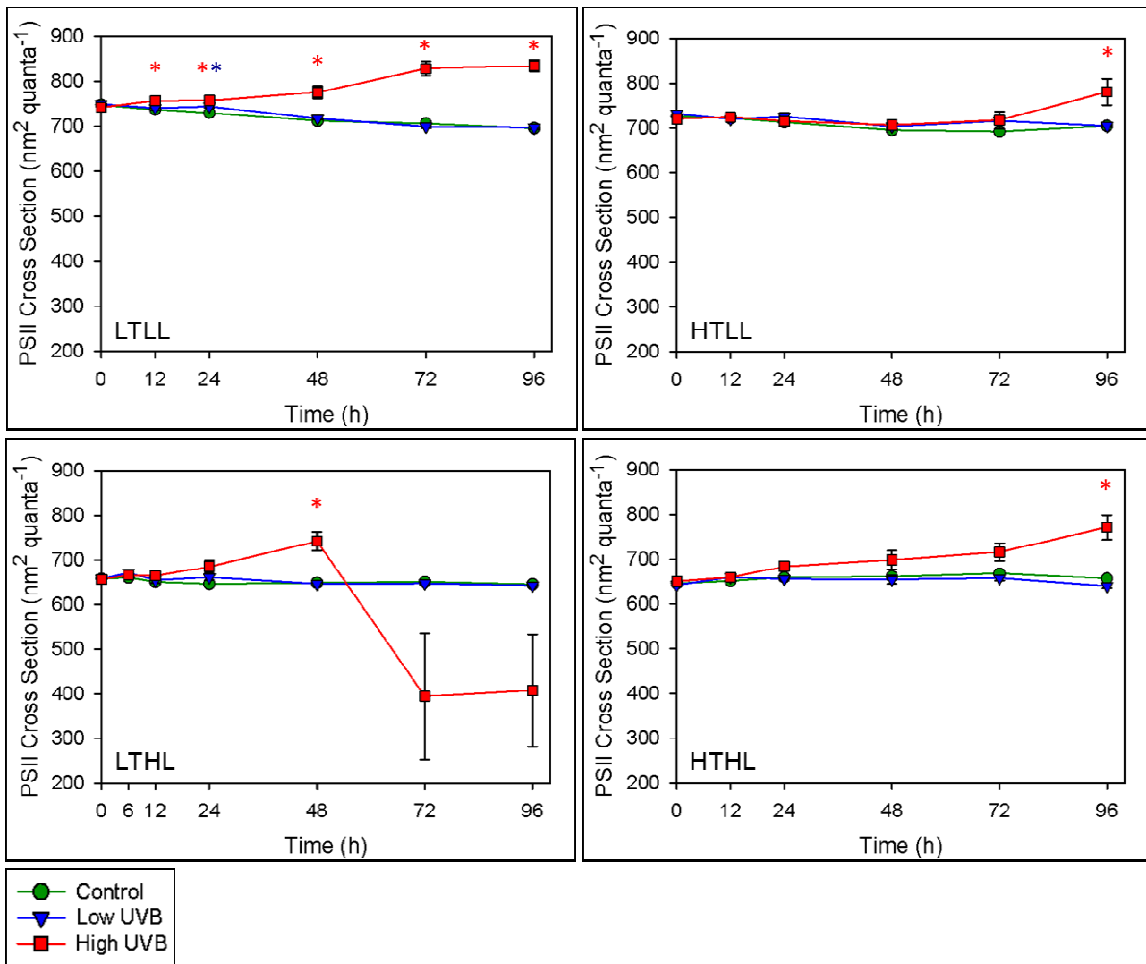
Figure 11. Mean cross-sectional area of photosystem II ($\pm$ standard error) for each of the four light and temperature experiments. Asterisks (*) represent significant differences (p<0.025) determined by Mann-Whitney-Wilcoxon tests between control and treatment represented by asterisk color.
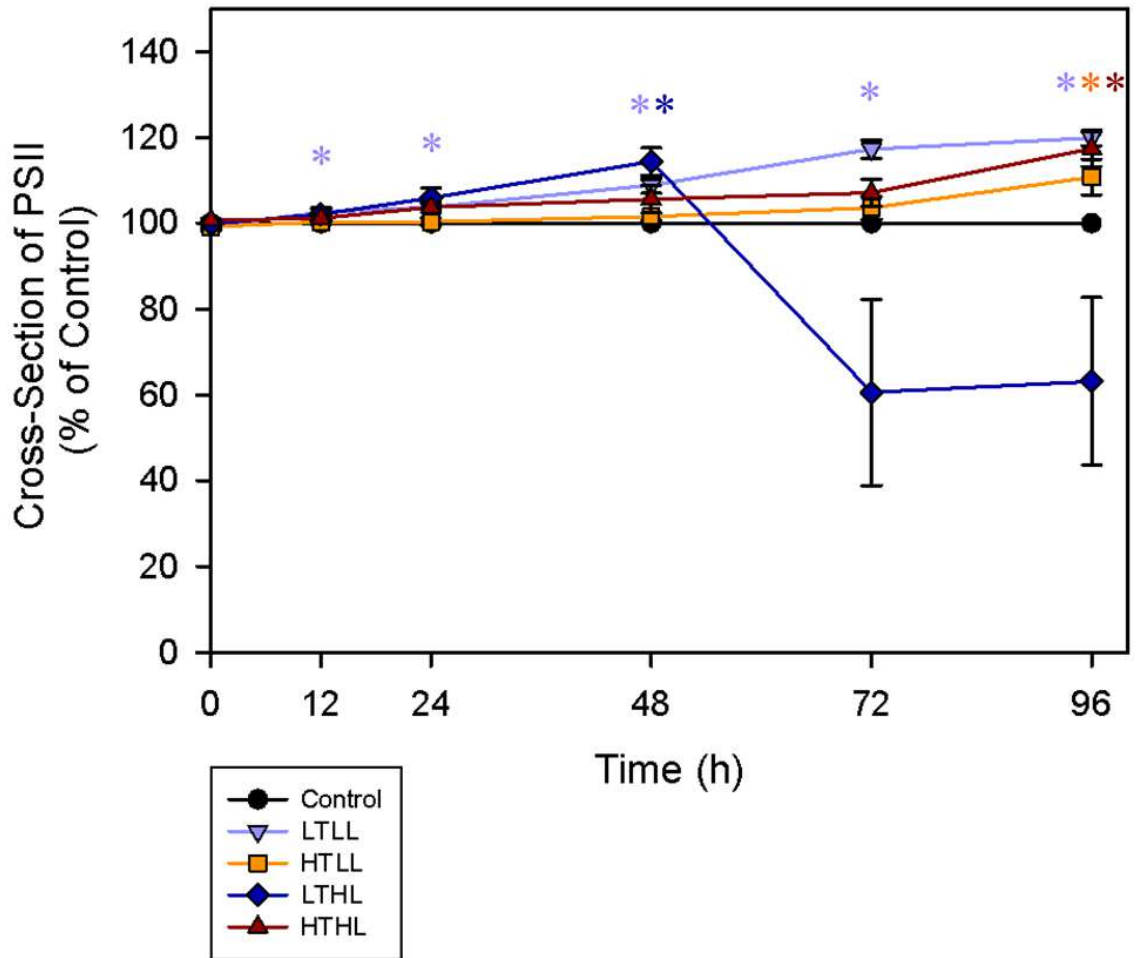
Figure 12. Mean cross-section of PSII ($\pm$ standard error) for each high UVB treatment normalized to the respective control treatment, shown as percent of the control treatment's cross-sectional area. The black bar represents the control value, at 100%. Asterisks (*) represent a significant difference between the high UVB treatment and its respective control, as determined by Mann-Whitney-Wilcoxon tests.
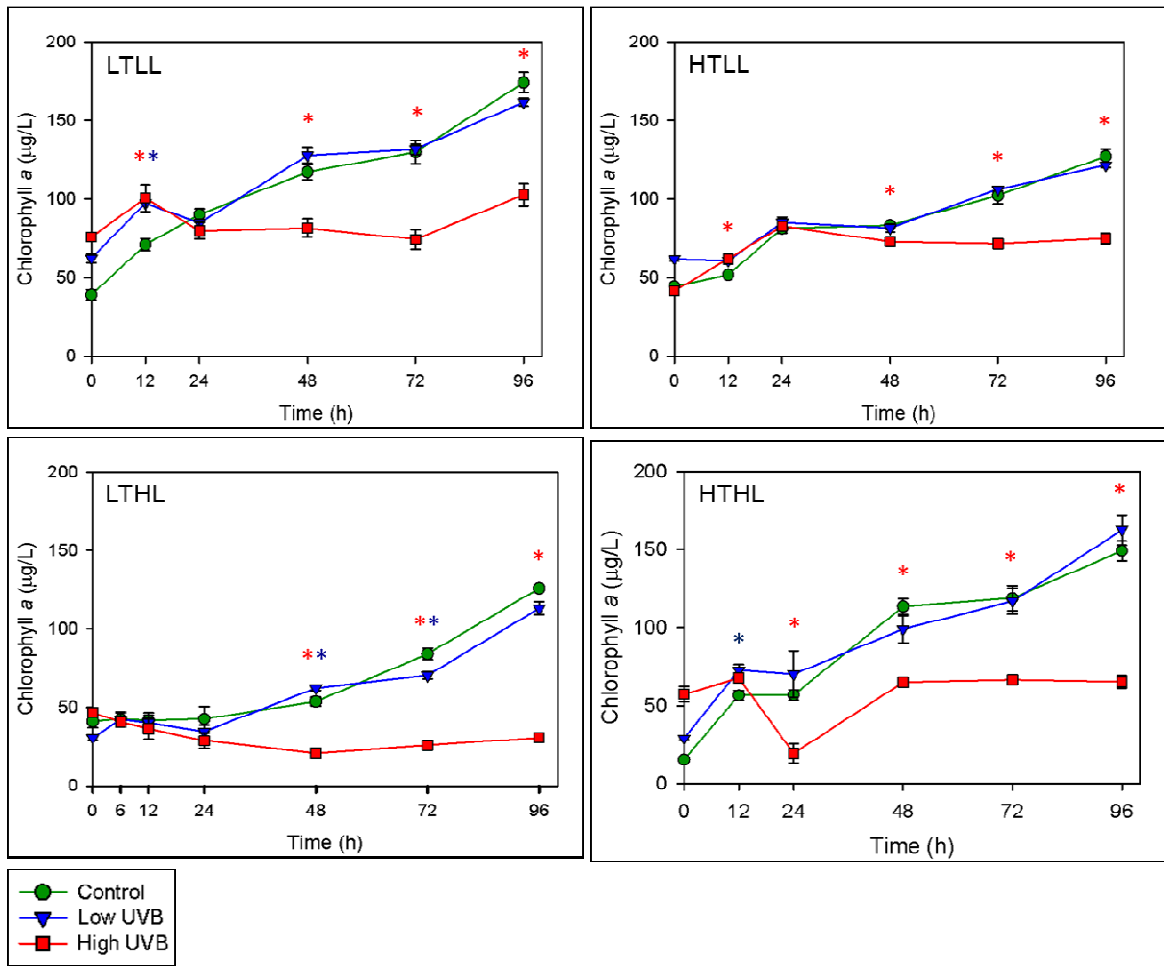
Figure 13. Mean chlorophyll *a* concentration (± standard error) for each of the four light and temperature experiments. Asterisks (*) represent significant differences (p<0.025) determined by Mann-Whitney-Wilcoxon tests between control and treatment represented by asterisk color.
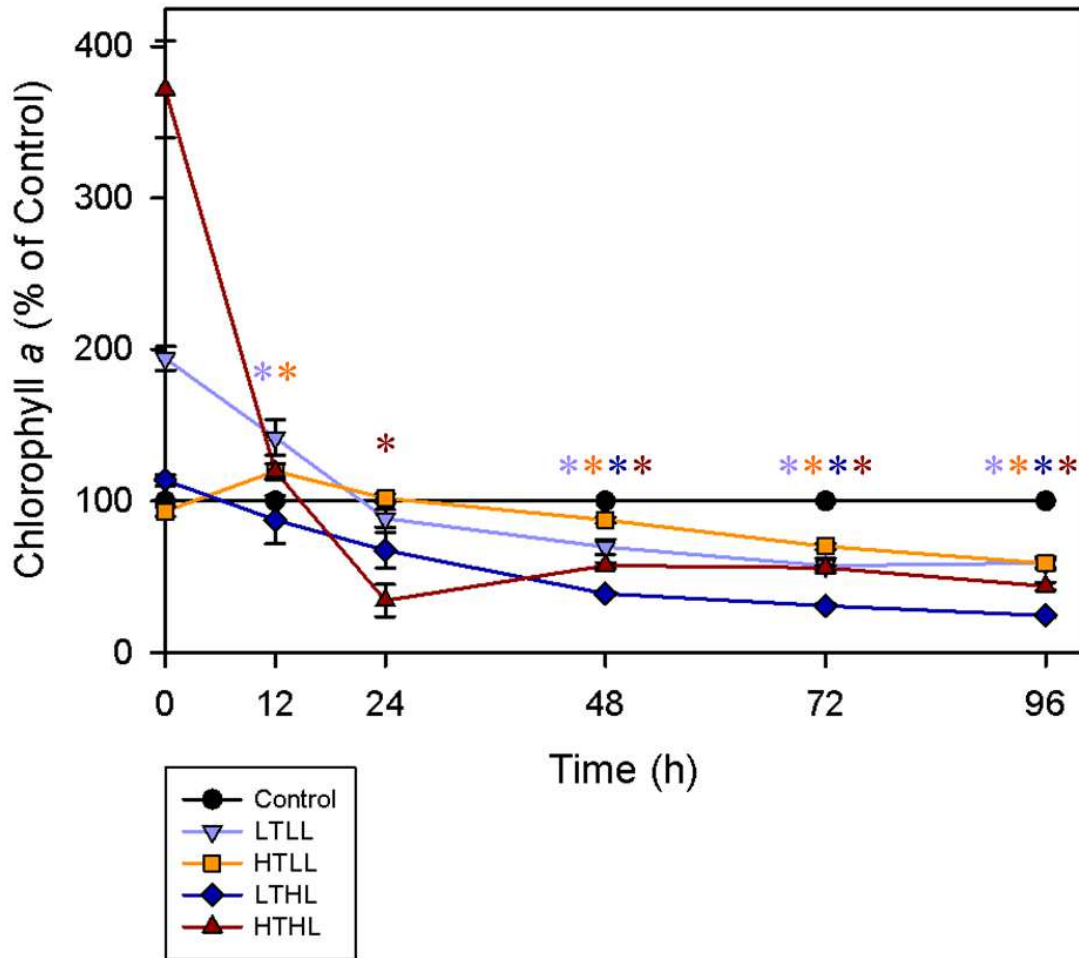
Figure 14. Mean chlorophyll *a* concentration (± standard error) for each high UVB treatment normalized to the respective control treatment, shown as percent of the control treatment's chlorophyll *a*. The black bar represents the control value, at 100%. Asterisks (*) represent a significant difference between the high UVB treatment and its respective control, as determined by Mann-Whitney-Wilcoxon tests.
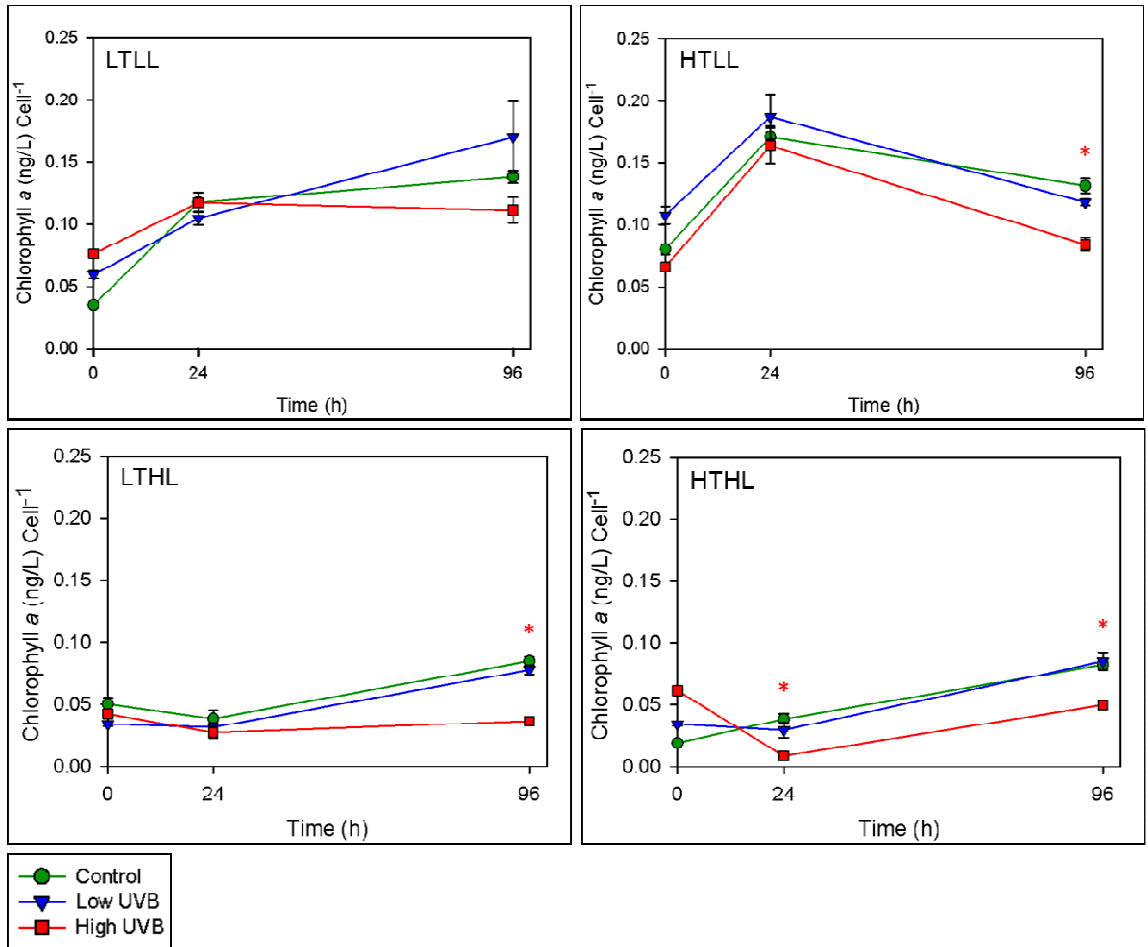
Figure 15. Mean chlorophyll *a* per cell (± standard error) for each of the four light and temperature experiments. Asterisks (*) represent significant differences (p<0.025) determined by Mann-Whitney-Wilcoxon tests between control and treatment represented by asterisk color.
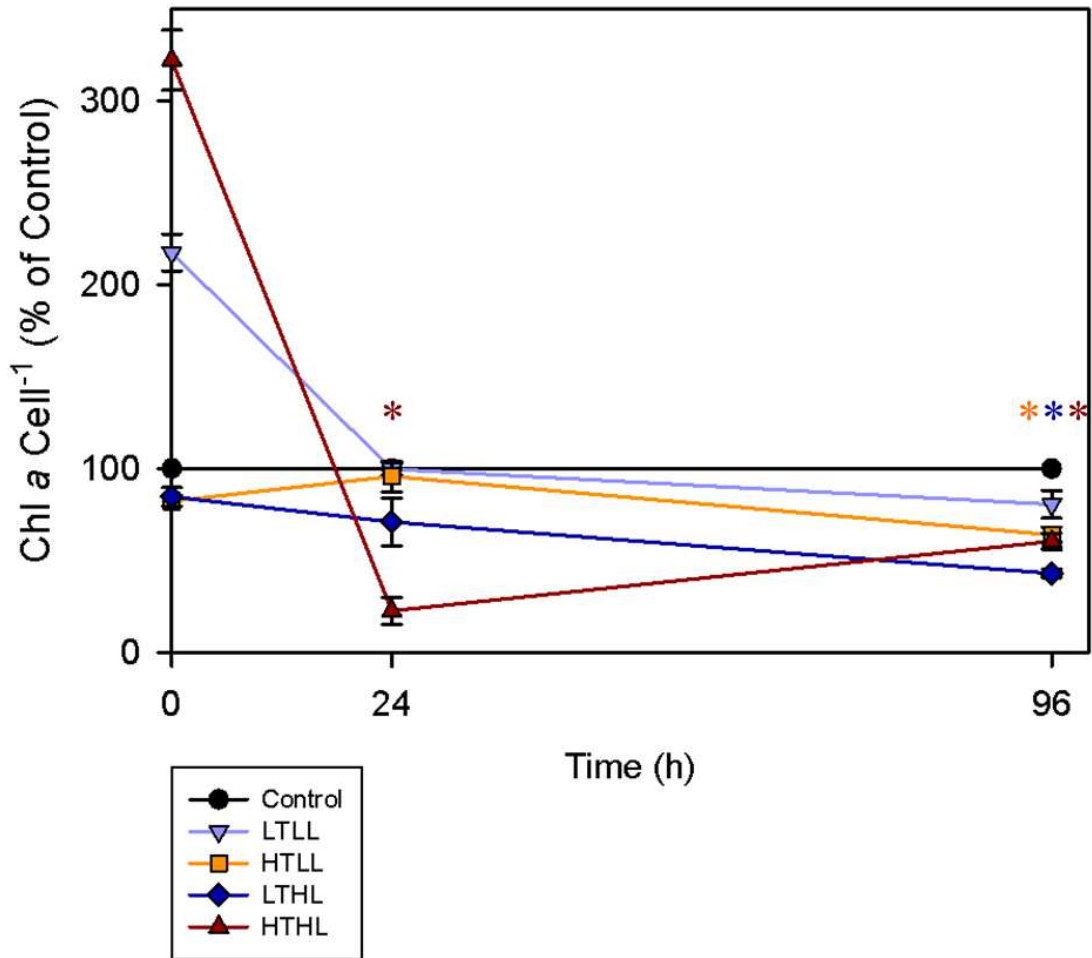
Figure 16. Mean chlorophyll *a* per cell ($\pm$ standard error) for each high UVB treatment normalized to the respective control treatment, shown as percent of the control treatment's chlorophyll *a* per cell. The black bar represents the control value, at 100%. Asterisks (*) represent a significant difference between the high UVB treatment and its respective control, as determined by Mann-Whitney-Wilcoxon tests.
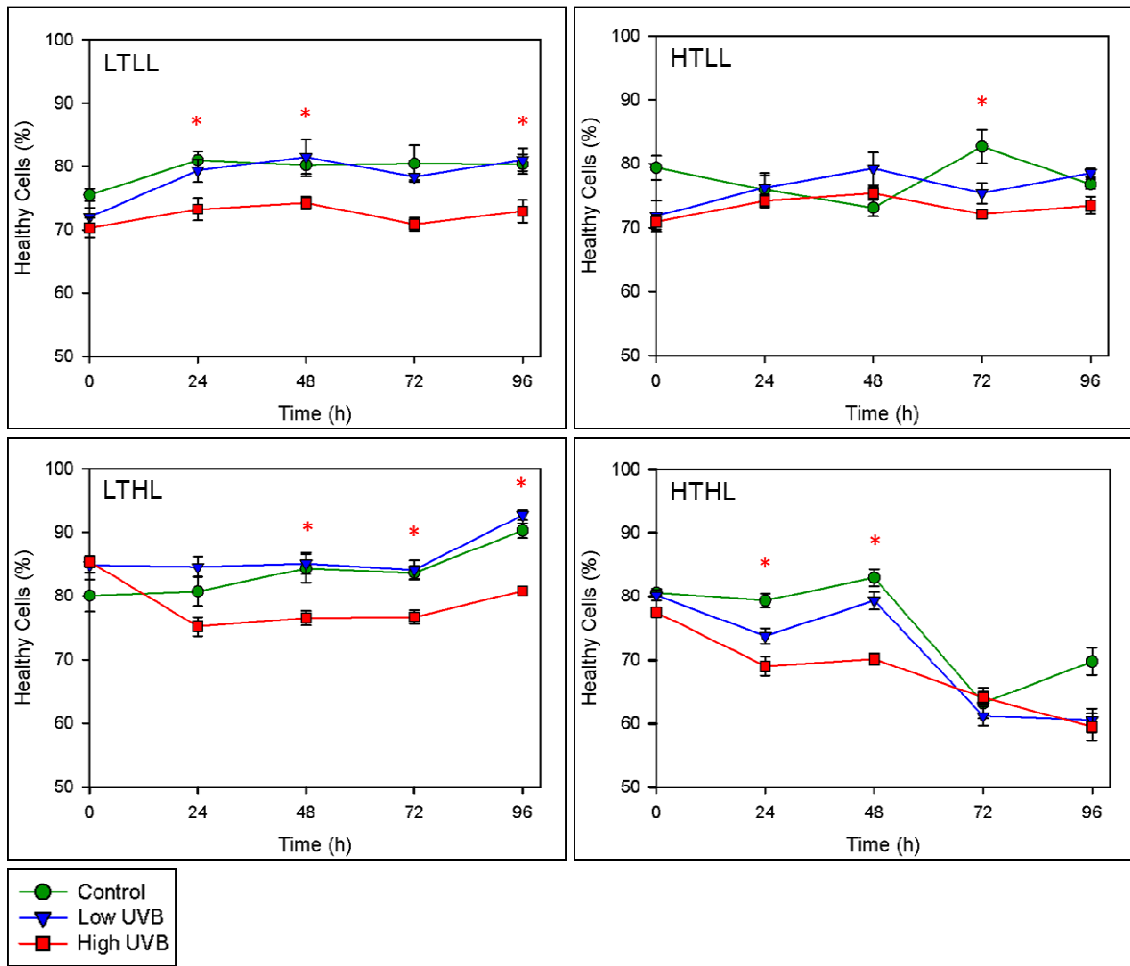
Figure 17. Mean percent of healthy cells (± standard error) for each of the four light and temperature experiments. Asterisks (*) represent significant differences (p<0.025) determined by Mann-Whitney-Wilcoxon tests between control and treatment represented by asterisk color.
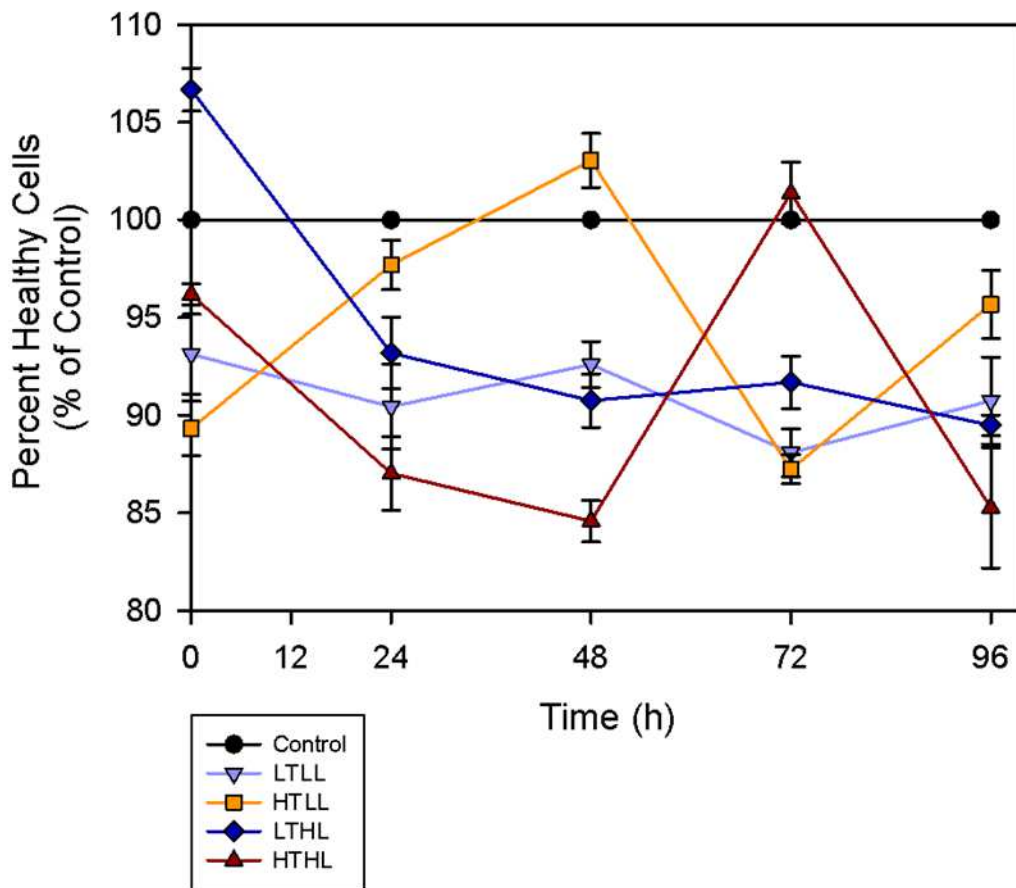
Figure 18. Mean percent of healthy cells ($\pm$ standard error) for each high UVB treatment normalized to the respective control treatment, shown as percent of the control treatment's chlorophyll *a* per cell. The black bar represents the control value, at 100%.
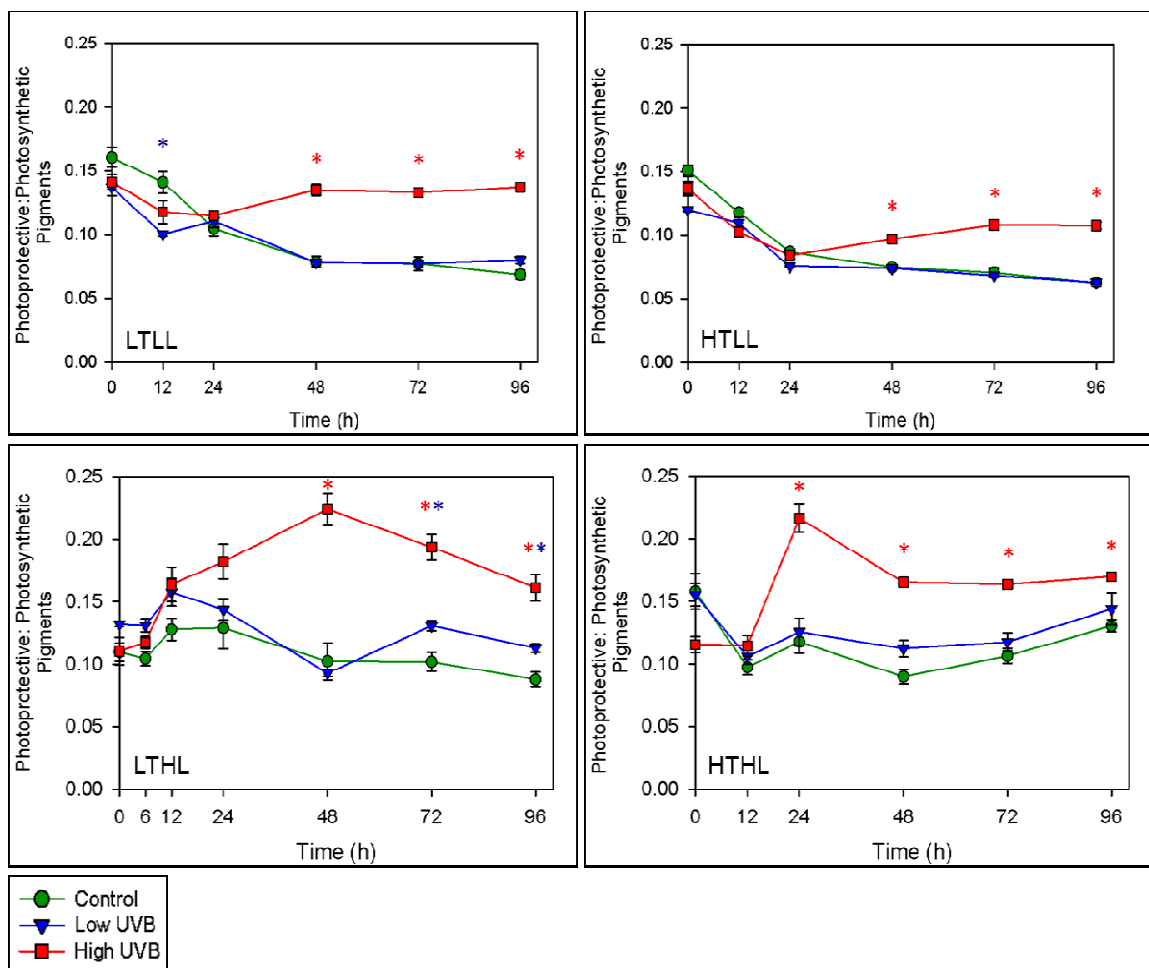
Figure 19. Mean relative concentration ($\pm$ standard error) of photoprotective (diadinoxanthin, diatoxanthin and β-carotene) to photosynthetic (chlorophyll *a*, chlorophyll c1, chlorophyll c2 and fucoxanthin) pigments for each of the four light and temperature experiments. Asterisks (*) represent significant differences (p<0.025) determined by Mann-Whitney-Wilcoxon tests between control and treatment represented by asterisk color.
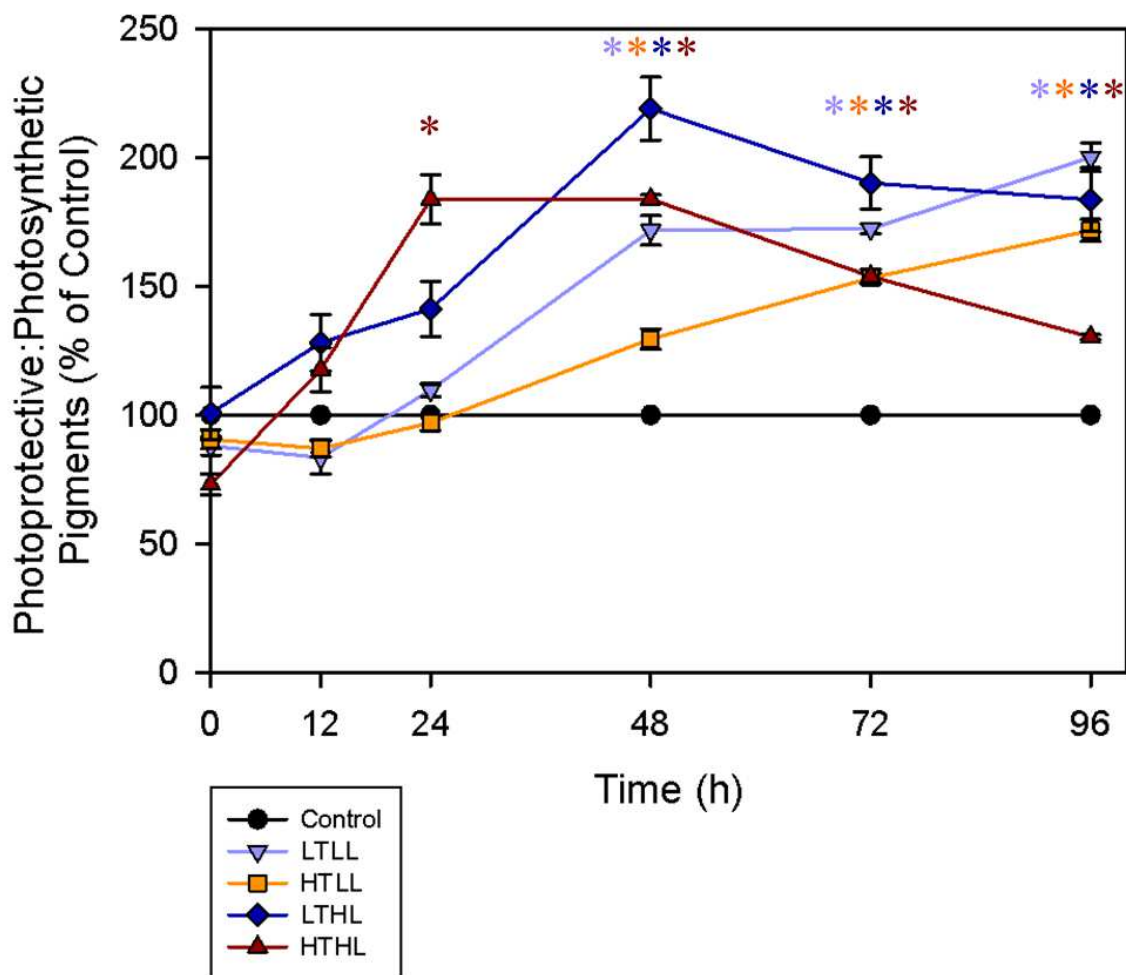
Figure 20. Mean relative concentration (± standard error) of photoprotective to photosynthetic pigments for each high UVB treatment normalized to the respective control treatment, shown as percent of the control treatment's ratio. The black bar represents the control value, at 100%. Asterisks (*) represent a significant difference between the high UVB treatment and its respective control, as determined by Mann-Whitney-Wilcoxon tests.
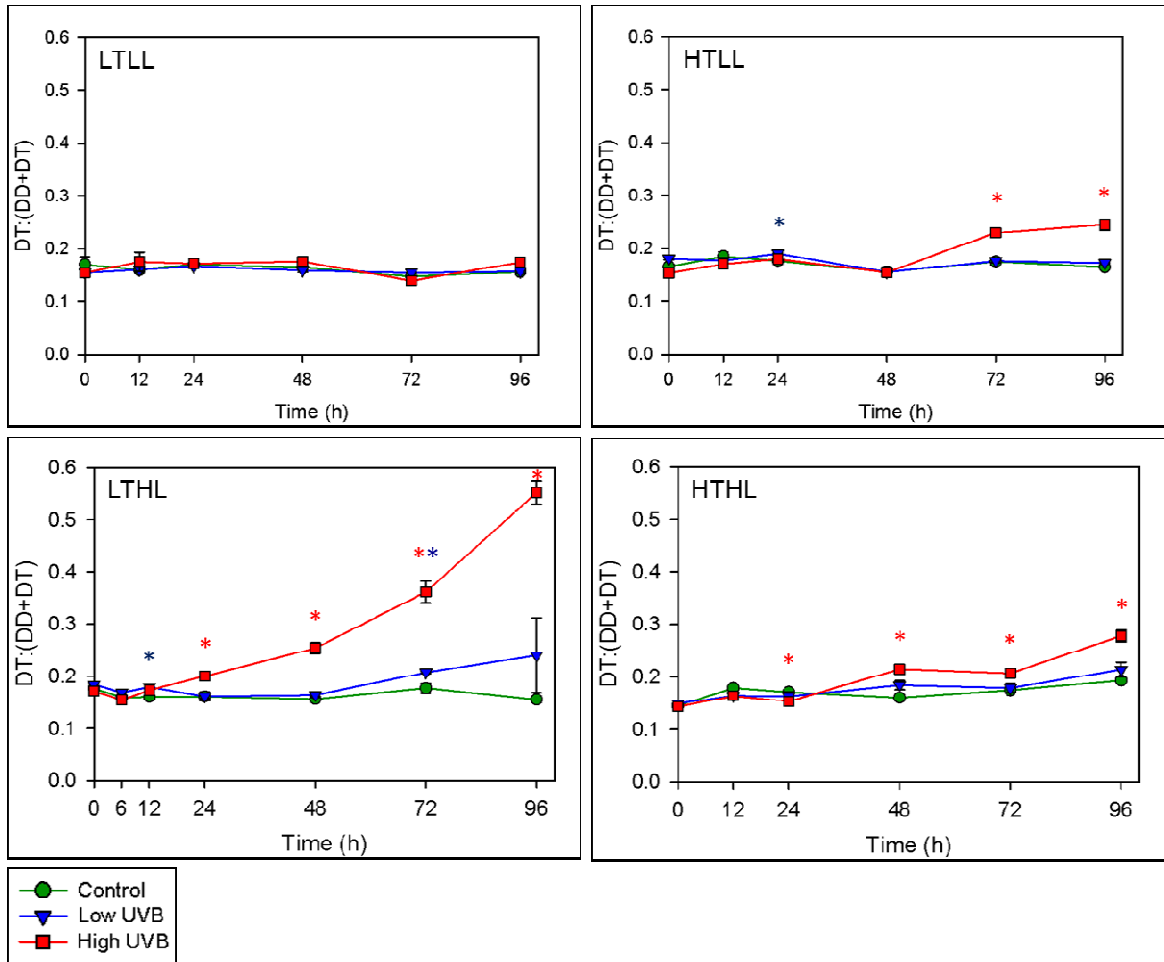
Figure 21. Mean xanthophyll cycling (± standard error) in each of the four light and temperature experiments. Asterisks (*) represent significant differences (p<0.025) determined by Mann-Whitney-Wilcoxon tests between control and treatment represented by asterisk color.
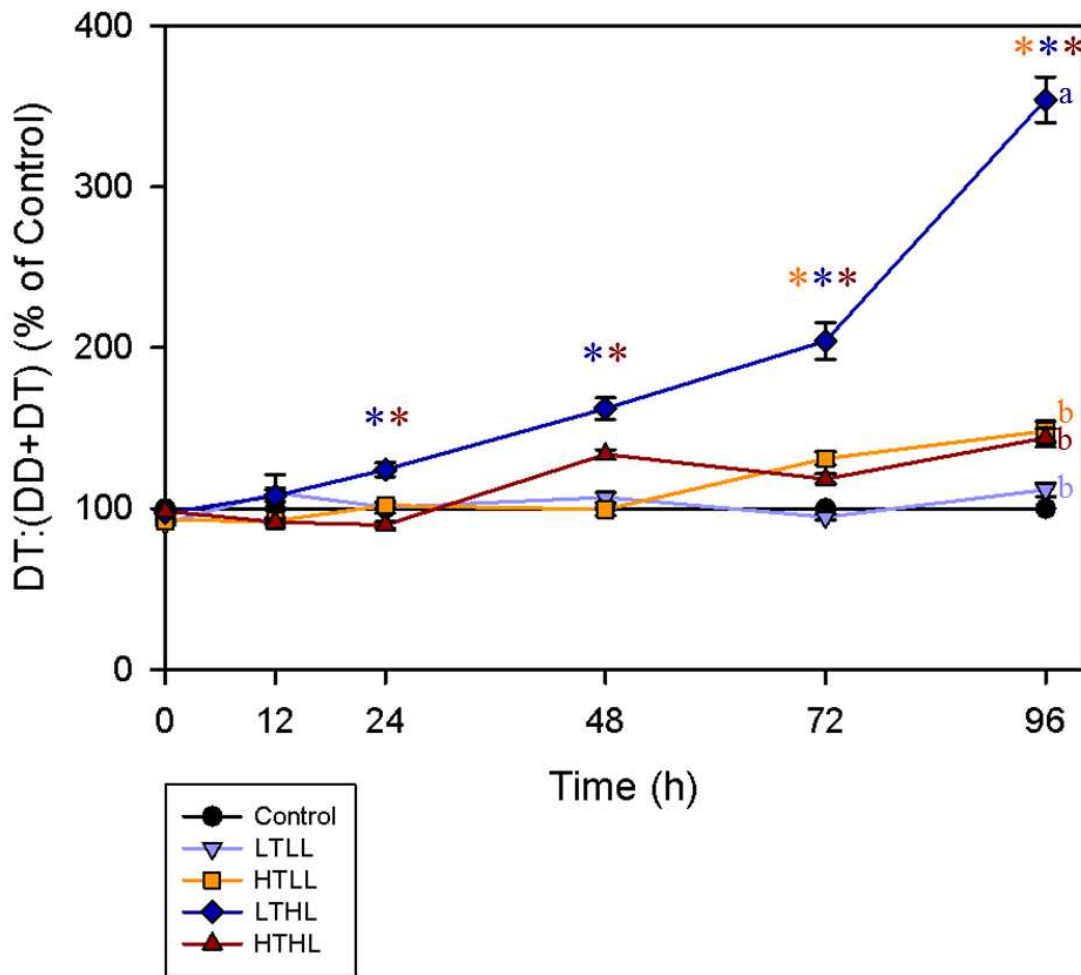
Figure 22. Mean xanthophyll cycling ($\pm$ standard error) (as DT:(DD+DT)) for each high UVB treatment normalized to the respective control treatment, shown as percent of the control treatment's DT:(DD+DT) ratio. The black bar represents the control value, at 100%. Asterisks (*) represent a significant difference between the high UVB treatment and its respective control, as determined by Mann-Whitney-Wilcoxon tests. Letters (a, b, etc.) represent significant difference among experiments, as determined by Tukey's post-hoc analysis.
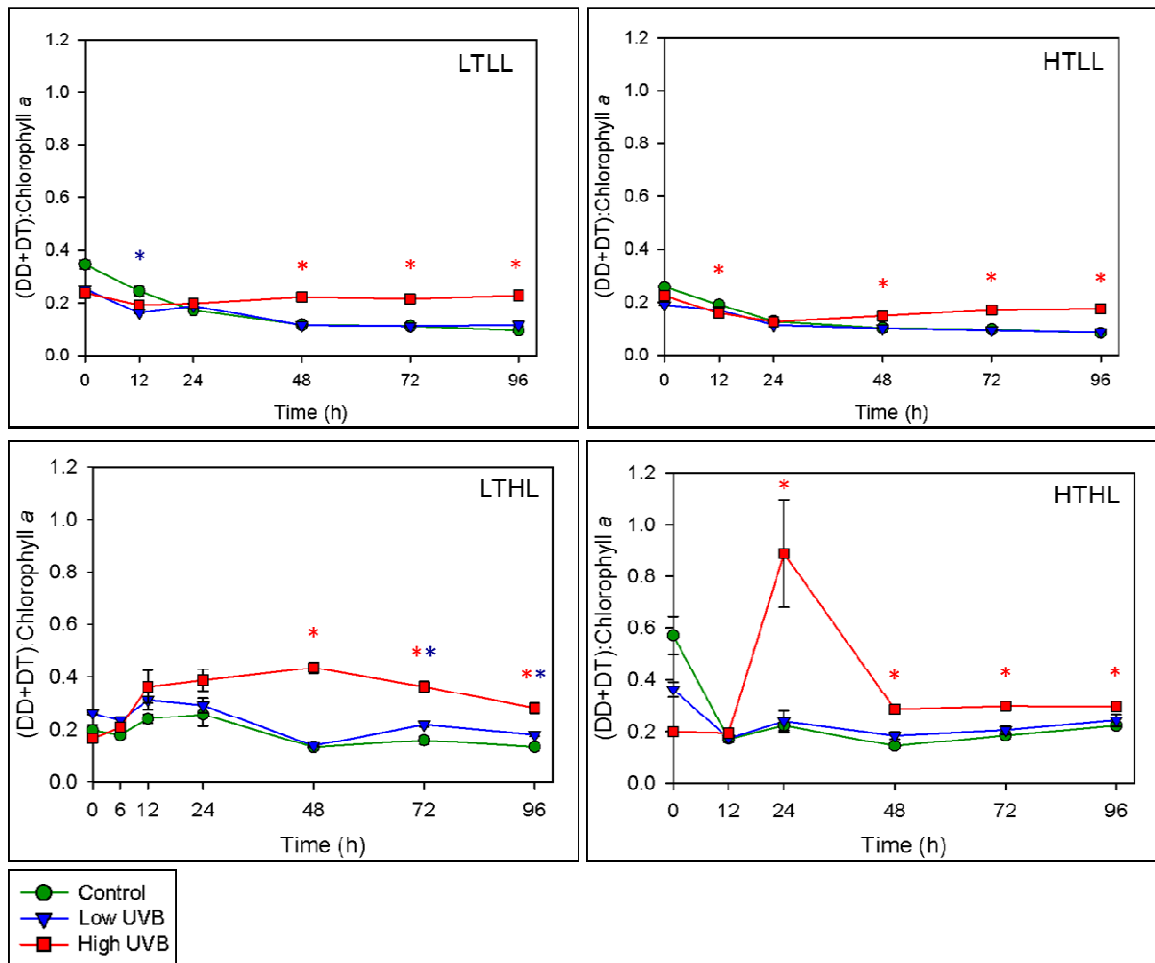
Figure 23. Mean relative concentration (+ standard error) of total xanthophyll pigments (diatoxanthin and diadinoxanthin) to chlorophyll *a* for each of the four light and temperature experiments. This ratio provides information on any change in the total pool of DD and DT. Asterisks (*) represent significant differences (p<0.025) determined by Mann-Whitney-Wilcoxon tests between control and treatment represented by asterisk color.
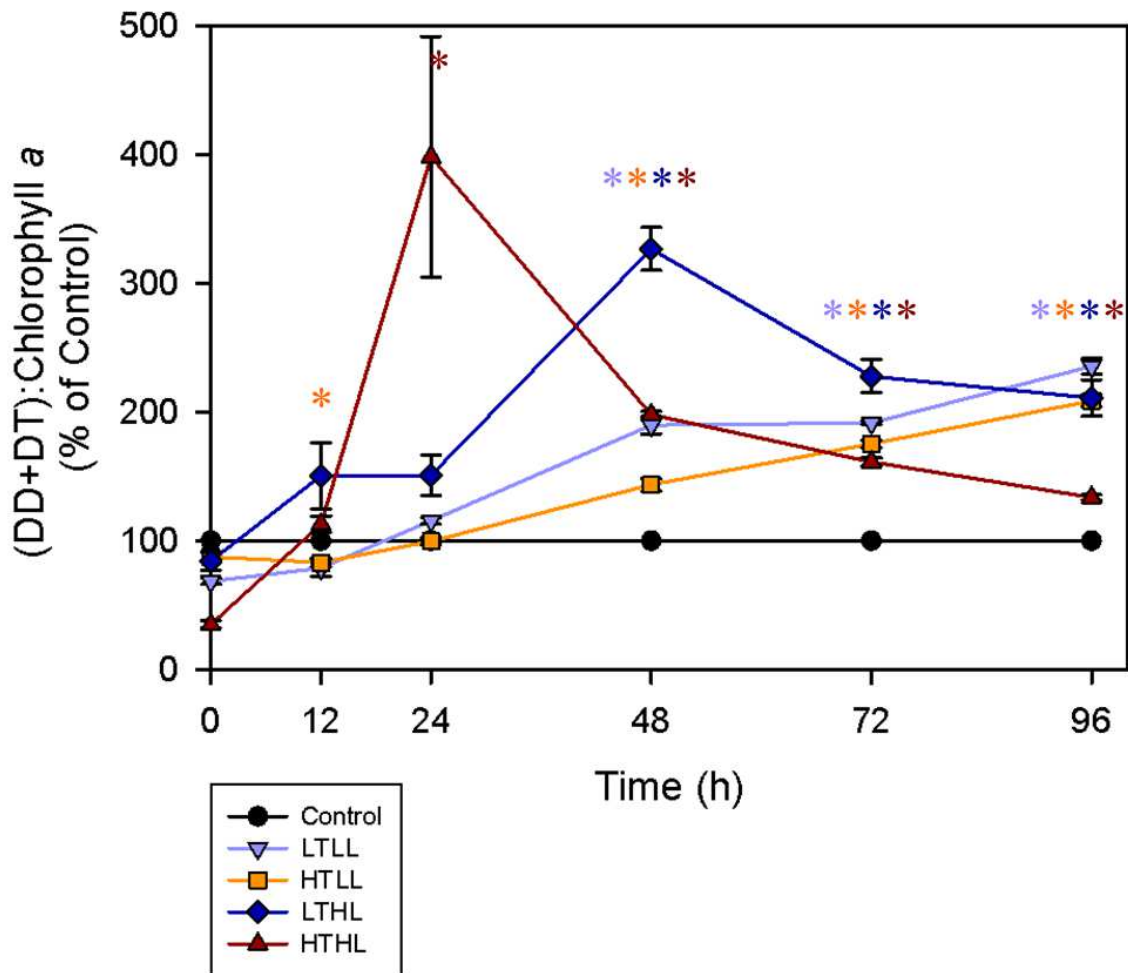
Figure 24. Mean total xanthophyll cycling pigment pool ($\pm$ standard error) for each high UVB treatment normalized to the respective control treatment, shown as percent of the control treatment's (DD+DT):Chl *a* ratio. The black bar represents the control value, at 100%. Asterisks (*) represent a significant difference between the high UVB treatment and its respective control, as determined by Mann-Whitney-Wilcoxon tests.
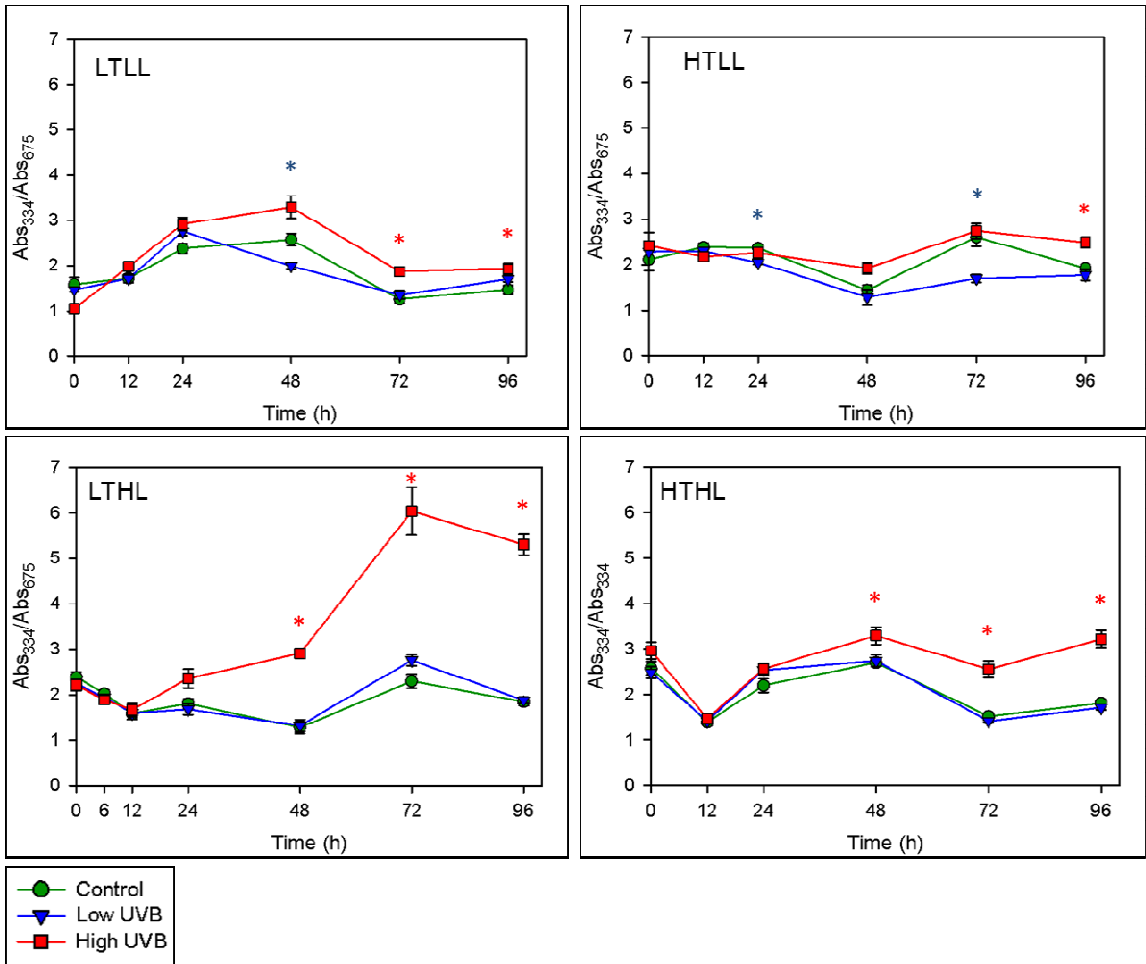
Figure 25. Mean absorbance at 334 nm ($\pm$ standard error) normalized to chlorophyll *a* absorbance at 675 nm for each of the light and temperature experiments. Asterisks (*) represent significant differences ($p<0.025$) determined by Mann-Whitney-Wilcoxon tests between control and treatment represented by asterisk color.
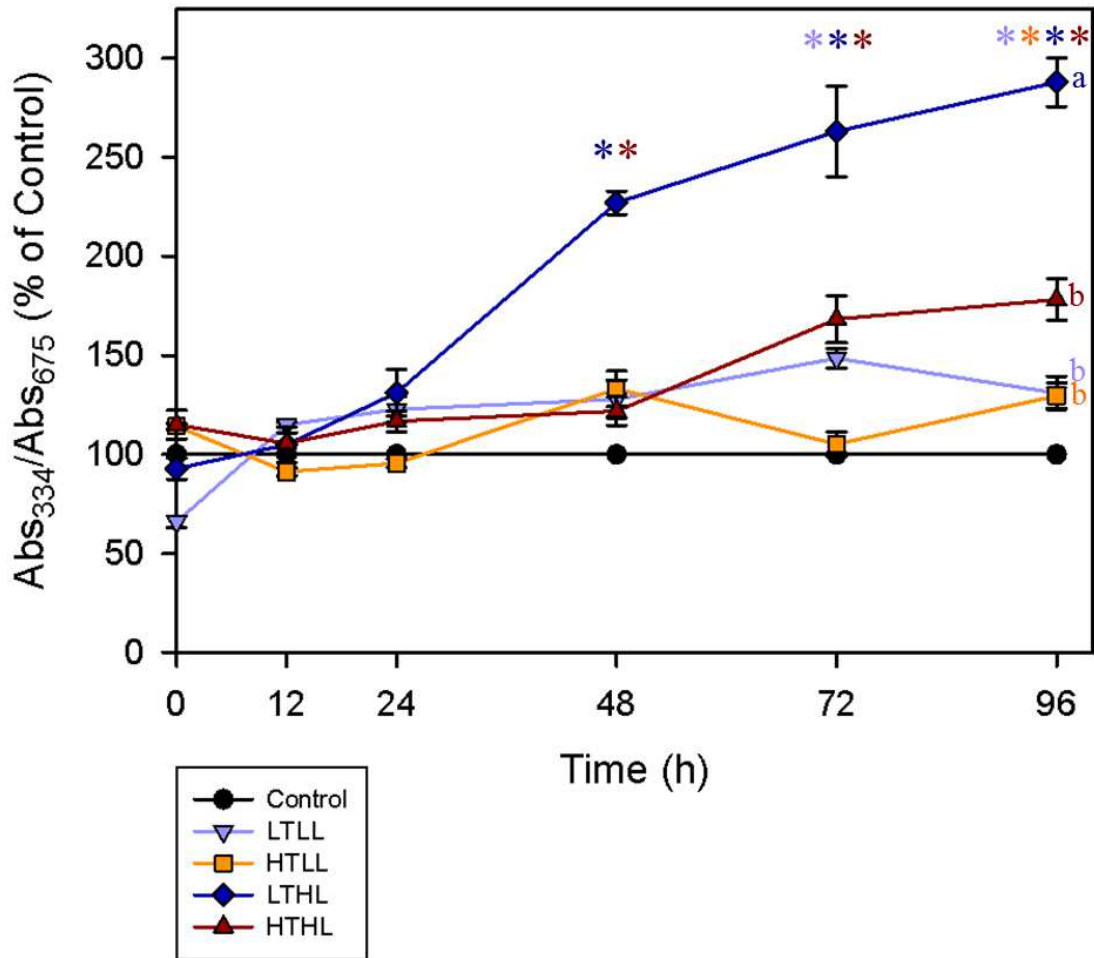
Figure 26. Mean Abs_{334}/Abs_{675} ($\pm$ standard error) for each high UVB treatment normalized to the respective control treatment, shown as percent of the control treatment's ratio. The black bar represents the control value, at 100%. Asterisks (*) represent a significant difference between the high UVB treatment and its respective control, as determined by Mann-Whitney-Wilcoxon tests. Letters (a, b, etc.) represent significant difference among experiments, as determined by Tukey's post-hoc analysis.

Tables

Table 1. PAR and UVB Irradiance for the UVB Treatments Under Each Light Condition

High Light Conditions	PAR (400-750 nm)	UVB (290-320 nm)	Percent UVB:Total
Control	3.3 W/m^2	3.9x10^{-4} W/m^2	0.01%
Low UV	2.9 W/m^2	4.1x10^{-3} W/m^2	0.14%
High UV	3.0 W/m^2	7.6x10^{-2} W/m^2	2.4%
Low Light Conditions			
Control	1.2 W/m^2	2.1x10^{-5} W/m^2	0.002%
Low UV	0.97 W/m^2	1.3x10^{-3} W/m^2	0.13%
High UV	1.2 W/m^2	2.3x10^{-2} W/m^2	1.9%

Table 2. Statistical Significance of Temperature and Light on Measured Variables.

	Temperature Significant at		Light Significant at		Temperature and Light Interaction
	Low Light	High Light	Low Temp	High Temp	
Cell Density	<0.001	<0.001	<0.001	<0.001	<0.001
Specific Growth Rate	<0.001	<0.001	<0.001	<0.001	NS
G1 phase	<0.001	NS	<0.05	<0.001	<0.001
S phase	<0.05	NS	<0.001	<0.001	<0.05
G2/M phase	NS	<0.05	<0.001	<0.001	NS
Fv/Fm	NS	NS	NS	NS	NS
Sigma	<0.001	<0.001	<0.001	<0.001	<0.001
Chlorophyll *a*	<0.001	<0.001	<0.001	NS	<0.001
Chl*a*:Cell	<0.05	<0.001	<0.05	<0.001	<0.001
DT:(DD+DT)	<0.001	<0.001	<0.001	NS	<0.001
(DD+DT):Chl*a*	<0.001	<0.001	<0.001	<0.001	<0.001
PP:PS Pigments	<0.001	NS	<0.001	<0.001	<0.05
B-car:Chl*a*	<0.001	NS	<0.05	NS	<0.05
Fuco:Chl*a*	<0.001	<0.001	<0.001	NS	<0.001
DD:Chl*a*	<0.05	<0.001	<0.001	NS	<0.001
DT:Chl*a*	<0.001	<0.001	<0.05	NS	NS
Abs_{334}/Abs_{675}	<0.05	NS	<0.001	<0.05	NS

Table 3. Mean ($\pm$ standard error) of Cell Density for All Temperature and Light Experiments. Significant Difference (p<0.05) from Control Denoted by Asterisk (*).

Environmental Conditions	UVB Treatment	Hour	Cell Density (mL^{-1})					
Low Temperature Low Light	Control	0	1,100,000$\pm$35,000	Low UVB	0	1,040,000$\pm$8,000	High UVB	0	990,000$\pm$11,000
		24	770,000$\pm$23,000		24	810,000$\pm$27,000		24	680,000$\pm$25,000*
		96	1,260,000$\pm$22,000		96	1,120,000$\pm$140,000		96	930,000$\pm$25,000*
High Temperature Low Light	Control	0	560,000$\pm$17,000	Low UVB	0	580,000$\pm$25,000	High UVB	0	610,000$\pm$31,000
		24	480,000$\pm$16,000		24	470,000$\pm$35,000		24	530,000$\pm$30,000
		96	970,000$\pm$11,000		96	1,030,000$\pm$12,000*		96	900,000$\pm$25,000*
Low Temperature High Light	Control	0	820,000$\pm$5,000	Low UVB	0	910,000$\pm$19,000	High UVB	0	1,110,000$\pm$44,000
		24	1,100,000$\pm$23,000		24	1,160,000$\pm$84,000		24	1,090,000$\pm$41,000
		96	1,500,000$\pm$72,000		96	1,460,000$\pm$30,000		96	850,000$\pm$20,000*
High Temperature High Light	Control	0	810,000$\pm$26,000	Low UVB	0	850,000$\pm$19,000	High UVB	0	910,000$\pm$50,000
		24	1,650,000$\pm$170,000		24	2,380,000$\pm$120,000		24	2,280,000$\pm$95,000
		96	1,810,000$\pm$24,000		96	1,930,000$\pm$62,000		96	1,380,000$\pm$30,000*

Table 4. Mean ($\pm$ standard error) of Photosynthetic Efficiency of Photosystem II for All Temperature and Light Experiments. Significant Difference ($p<0.05$) from Control Denoted by Asterisk (*).

Environmental Conditions	UVB Treatment	Hour	Photosynthetic Efficiency of PSII (Fv/Fm)					
Low Temperature Low Light	Control	0	0.423 ± 0.001	Low UVB	0	0.421 ± 0.003	High UVB	0	0.417 ± 0.002
		12	0.448 ± 0.003		12	0.438 ± 0.005		12	$0.423\pm0.002*$
		24	0.442 ± 0.005		24	0.435 ± 0.006		24	$0.390\pm0.006*$
		48	0.472 ± 0.003		48	0.467 ± 0.002		48	$0.302\pm0.013*$
		72	0.477 ± 0.004		72	0.471 ± 0.003		72	$0.203\pm0.006*$
		96	0.490 ± 0.004		96	0.480 ± 0.008		96	$0.144\pm0.013*$
High Temperature Low Light	Control	0	0.406 ± 0.004	Low UVB	0	0.397 ± 0.012	High UVB	0	0.409 ± 0.002
		12	0.429 ± 0.004		12	0.423 ± 0.005		12	0.413 ± 0.005
		24	0.435 ± 0.003		24	0.435 ± 0.003		24	0.419 ± 0.007
		48	0.472 ± 0.004		48	0.457 ± 0.007		48	$0.405\pm0.004*$
		72	0.478 ± 0.008		72	0.478 ± 0.001		72	$0.318\pm0.014*$
		96	0.479 ± 0.006		96	0.472 ± 0.004		96	$0.204\pm0.013*$
Low Temperature High Light	Control	0	0.481 ± 0.005	Low UVB	0	0.455 ± 0.005	High UVB	0	0.455 ± 0.007
		12	0.476 ± 0.005		12	0.461 ± 0.002		12	$0.420\pm0.006*$
		24	0.481 ± 0.004		24	0.470 ± 0.002		24	$0.337\pm0.015*$
		48	0.493 ± 0.002		48	0.476 ± 0.008		48	$0.091\pm0.010*$
		72	0.480 ± 0.007		72	0.473 ± 0.005		72	$0.024\pm0.005*$
		96	0.481 ± 0.008		96	0.486 ± 0.003		96	$0.021\pm0.009*$
High Temperature High Light	Control	0	0.463 ± 0.002	Low UVB	0	0.461 ± 0.002	High UVB	0	0.462 ± 0.002
		12	0.473 ± 0.004		12	0.461 ± 0.004		12	$0.435\pm0.005*$
		24	0.479 ± 0.002		24	0.463 ± 0.005		24	$0.375\pm0.014*$
		48	0.481 ± 0.004		48	0.467 ± 0.004		48	$0.230\pm0.021*$
		72	0.481 ± 0.003		72	0.479 ± 0.001		72	$0.157\pm0.018*$
		96	0.482 ± 0.002		96	0.468 ± 0.005		96	$0.083\pm0.021*$

Table 5. Mean ($\pm$ standard error) of Cross-Sectional Area of Photosystem II for All Temperature and Light Experiments. Significant Difference (p<0.05) from Control Denoted by Asterisk (*).

Environmental Conditions	UVB Treatment	Hour	Cross-Sectional Area of PSII (nm^2 quanta^{-1})					
Low Temperature Low Light	Control	0	746.2$\pm$6.8	Low UVB	0	744.2$\pm$5.8	High UVB	0	739.0$\pm$4.9
		12	736.9$\pm$4.0		12	747.4$\pm$8.1		12	755.1$\pm$4.3
		24	729.2$\pm$2.6		24	744.0$\pm$3.4*		24	759.1$\pm$4.8*
		48	711.1$\pm$3.9		48	718.6$\pm$2.2		48	775.3$\pm$13.6*
		72	704.0$\pm$4.5		72	698.6$\pm$3.5		72	829.0$\pm$12.9*
		96	695.7$\pm$3.1		96	696.8$\pm$3.3		96	834.1$\pm$12.6*
High Temperature Low Light	Control	0	727.8$\pm$3.6	Low UVB	0	728.8$\pm$4.3	High UVB	0	722.1$\pm$5.7
		12	721.8$\pm$3.0		12	719.7$\pm$4.9		12	725.4$\pm$3.9
		24	706.5$\pm$3.3		24	723.8$\pm$6.6		24	718.0$\pm$6.0
		48	689.6$\pm$1.8		48	700.4$\pm$5.0		48	705.6$\pm$4.8
		72	694.6$\pm$5.6		72	718.6$\pm$4.5		72	710.0$\pm$16.7
		96	704.6$\pm$3.4		96	703.0$\pm$2.5		96	777.8$\pm$24.0*
Low Temperature High Light	Control	0	659.1$\pm$4.6	Low UVB	0	655.9$\pm$3.0	High UVB	0	656.5$\pm$5.9
		12	650.1$\pm$3.4		12	655.0$\pm$4.9		12	664.5$\pm$9.3
		24	648.6$\pm$4.1		24	658.4$\pm$5.6		24	688.8$\pm$12.9*
		48	649.8$\pm$5.8		48	646.5$\pm$3.2		48	737.5$\pm$17.4*
		72	651.7$\pm$3.8		72	647.0$\pm$2.9		72	418.4$\pm$117.6
		96	645.5$\pm$5.5		96	642.3$\pm$3.1		96	407.7$\pm$126.0
High Temperature High Light	Control	0	643.4$\pm$3.7	Low UVB	0	640.6$\pm$3.2	High UVB	0	654.0$\pm$4.3
		12	649.6$\pm$3.1		12	657.2$\pm$4.2		12	660.5$\pm$5.2
		24	661.1$\pm$3.1		24	654.4$\pm$3.1		24	684.3$\pm$6.1*
		48	662.1$\pm$6.3		48	654.5$\pm$9.6		48	695.0$\pm$17.7
		72	668.3$\pm$4.6		72	657.1$\pm$4.1		72	698.7$\pm$8.4*
		96	654.7$\pm$5.4		96	645.1$\pm$2.0		96	756.8$\pm$26.8*

Table 6. Mean (± standard error) of Chlorophyll *a* Concentration for All Temperature and Light Experiments. Significant Difference (p<0.05) from Control Denoted by Asterisk (*).

Environmental Conditions	UVB Treatment	Hour	Chlorophyll *a*(μg/L)					
Low Temperature Low Light	Control	0	40.4+2.9	Low UVB	0	62.8+2.6	High UVB	0	72.8+0.4
		12	71.0+3.8		12	94.5+6.3*		12	96.2+8.2*
		24	90.2+3.6		24	84.6+2.3		24	81.2+4.9
		48	116.2+4.1		48	124.7+5.1		48	81.5+5.8*
		72	134.4+7.5		72	133.3+3.1		72	74.4+5.1*
		96	174.1+6.4		96	161.6+2.6		96	94.6+1.4*
High Temperature Low Light	Control	0	44.8+0.9	Low UVB	0	61.5+1.4	High UVB	0	41.5+1.2
		12	50.6+1.5		12	60.5+2.1*		12	62.0+2.6*
		24	79.4+3.1		24	83.9+3.0		24	83.2+2.0
		48	83.0+1.2		48	82.7+2.3		48	72.8+1.5*
		72	99.9+5.0		72	107.3+1.5		72	69.7+2.6*
		96	127.2+4.6		96	121.5+1.7		96	74.9+3.3*
Low Temperature High Light	Control	0	40.4+3.4	Low UVB	0	30.6+1.3	High UVB	0	46.7+1.5
		12	39.0+4.8		12	37.6+4.8		12	36.4+6.6
		24	36.4+8.9		24	34.6+4.3		24	27.7+4.2
		48	53.8+2.8		48	62.4+1.3*		48	21.3+0.6*
		72	73.7+10.8		72	67.0+3.8*		72	25.8+1.0*
		96	125.9+1.9		96	113.2+4.1*		96	30.9+1.0*
High Temperature High Light	Control	0	15.5+0.7	Low UVB	0	28.5+1.0	High UVB	0	57.5+4.9
		12	61.1+5.6		12	69.1+5.2		12	67.7+3.0
		24	57.1+2.8		24	64.5+13.3		24	27.8+9.7*
		48	113.9+4.0		48	99.1+8.6*		48	65.8+1.8*
		72	119.0+8.0		72	119.0+7.0		72	67.5+1.8*
		96	147.5+5.5		96	158.1+9.1		96	66.4+3.4*

Table 7. Mean (± standard error) of Chlorophyll *a* Per Cell for All Temperature and Light Experiments. Significant Difference (p<0.05) from Control Denoted by Asterisk (*).

Environmental Conditions	UVB Treatment	Hour	Chlorophyll *a* per cell						
Low Temperature Low Light	Control	0	0.037±0.002	Low UVB	0	0.060±0.003	High UVB	0	0.073±0.002
		24	0.118±0.008		24	0.105±0.006		24	0.118±0.003
		96	0.138±0.005		96	0.170±0.029		96	0.102±0.002*
High Temperature Low Light	Control	0	0.080±0.004	Low UVB	0	0.108±0.007	High UVB	0	0.068±0.003
		24	0.166±0.008		24	0.182±0.015		24	0.159±0.012
		96	0.132±0.006		96	0.118±0.003		96	0.084±0.005*
Low Temperature High Light	Control	0	0.050±0.004	Low UVB	0	0.034±0.002	High UVB	0	0.042±0.003
		24	0.033±0.005		24	0.027+0.003		24	0.022±0.004
		96	0.059±0.003		96	0.054±0.001		96	0.023±0.002*
High Temperature High Light	Control	0	0.019±0.001	Low UVB	0	0.034±0.001	High UVB	0	0.061±0.003
		24	0.036±0.004		24	0.027±0.006		24	0.012±0.004*
		96	0.060±0.002		96	0.062±0.005		96	0.036±0.002*

Table 8. Mean ($\pm$ standard error) of Xanthophyll Cycling for All Temperature and Light Experiments. Significant Difference ($p<0.05$) from Control Denoted by Asterisk (*).

Environmental Conditions	UVB Treatment	Hour	DT:(DD+DT)					
Low Temperature Low Light	Control	0	0.157$\pm$0.002	Low UVB	0	0.158$\pm$0.005	High UVB	0	0.157$\pm$0.002
		12	0.160$\pm$0.003		12	0.162$\pm$0.005		12	0.172$\pm$0.015
		24	0.171$\pm$0.006		24	0.166$\pm$0.003		24	0.173$\pm$0.005
		48	0.164$\pm$0.004		48	0.159$\pm$0.003		48	0.176$\pm$0.005
		72	0.148$\pm$0.006		72	0.155$\pm$0.001		72	0.140$\pm$0.002
		96	0.157$\pm$0.005		96	0.153$\pm$0.002		96	0.175$\pm$0.007
High Temperature Low Light	Control	0	0.169$\pm$0.002	Low UVB	0	0.182$\pm$0.002	High UVB	0	0.153$\pm$0.002
		12	0.185$\pm$0.007		12	0.173$\pm$0.002		12	0.171$\pm$0.004
		24	0.177$\pm$0.002		24	0.190$\pm$0.001		24	0.180$\pm$0.003
		48	0.156$\pm$0.003		48	0.157$\pm$0.002		48	0.155$\pm$0.006
		72	0.176$\pm$0.005		72	0.176$\pm$0.003		72	0.237$\pm$0.009*
		96	0.165$\pm$0.004		96	0.174$\pm$0.001		96	0.239$\pm$0.010*
Low Temperature High Light	Control	0	0.177$\pm$0.002	Low UVB	0	0.184$\pm$0.002	High UVB	0	0.172$\pm$0.004
		12	0.164$\pm$0.005		12	0.184$\pm$0.006		12	0.173$\pm$0.006
		24	0.163$\pm$0.007		24	0.160$\pm$0.004		24	0.202$\pm$0.006*
		48	0.162$\pm$0.006		48	0.164$\pm$0.004		48	0.252$\pm$0.009*
		72	0.188$\pm$0.013		72	0.209$\pm$0.002*		72	0.366$\pm$0.017*
		96	0.156$\pm$0.006		96	0.168$\pm$0.001		96	0.548$\pm$0.020*
High Temperature High Light	Control	0	0.146$\pm$0.002	Low UVB	0	0.151$\pm$0.003	High UVB	0	0.143$\pm$0.001
		12	0.180$\pm$0.003		12	0.166$\pm$0.004		12	0.164$\pm$0.003
		24	0.169$\pm$0.004		24	0.162$\pm$0.007		24	0.157$\pm$0.004
		48	0.160$\pm$0.005		48	0.184$\pm$0.009*		48	0.221$\pm$0.008*
		72	0.175$\pm$0.005		72	0.180$\pm$0.007		72	0.207$\pm$0.004*
		96	0.190$\pm$0.006		96	0.214$\pm$0.011		96	0.276$\pm$0.009*

Table 9. Mean (± standard error) of Total Xanthophyll Cycling Pigment Pool for All Temperature and Light Experiments. Significant Difference (p<0.05) from Control Denoted by Asterisk (*).

Environmental Conditions	UVB Treatment	Hour	(DT+DD): Chlorophyll *a*					
Low Temperature Low Light	Control	0	0.350±0.015	Low UVB	0	0.246±0.011	High UVB	0	0.240±0.007
		12	0.244±0.017		12	0.162±0.003*		12	0.197±0.014
		24	0.171±0.011		24	0.187±0.011		24	0.198±0.005
		48	0.121±0.008		48	0.116±0.004		48	0.222±0.008*
		72	0.109±0.008		72	0.112±0.002		72	0.215±0.001*
		96	0.096±0.006		96	0.144±0.005*		96	0.227±0.006*
High Temperature Low Light	Control	0	0.255±0.007	Low UVB	0	0.189±0.001	High UVB	0	0.223±0.009
		12	0.194±0.006		12	0.165±0.008*		12	0.149±0.010*
		24	0.127±0.003		24	0.114±0.001		24	0.125±0.003
		48	0.102±0.002		48	0.102±0.001		48	0.146±0.004*
		72	0.098±0.005		72	0.096±0.002		72	0.175±0.004*
		96	0.084±0.005		96	0.087±0.002		96	0.172±0.005*
Low Temperature High Light	Control	0	0.188±0.019	Low UVB	0	0.263±0.003	High UVB	0	0.166±0.014
		12	0.267±0.029		12	0.341±0.046		12	0.363±0.062
		24	0.237±0.041		24	0.292±0.025		24	0.404±0.037*
		48	0.133±0.011		48	0.139±0.004		48	0.419±0.024*
		72	0.203±0.045		72	0.231±0.016*		72	0.363±0.019*
		96	0.134±0.010		96	0.181±0.005*		96	0.284±0.016*
High Temperature High Light	Control	0	0.572±0.074	Low UVB	0	0.365±0.024	High UVB	0	0.200±0.017
		12	0.170±0.012		12	0.185±0.014		12	0.194±0.011
		24	0.220±0.016		24	0.249±0.036		24	0.782±0.201*
		48	0.142±0.008		48	0.184±0.013*		48	0.290±0.005*
		72	0.185±0.013		72	0.209±0.013		72	0.295±0.006*
		96	0.217±0.010		96	0.257±0.024		96	0.301±0.006*

Table 10. Mean ($\pm$ standard error) of Photoprotective to Photosynthetic Pigments for All Temperature and Light Experiments. Significant Difference ($p<0.05$) from Control Denoted by Asterisk (*).

Environmental Conditions	UVB Treatment	Hour	Photoprotective:Photosynthetic Pigments					
Low Temperature Low Light	Control	0	0.161+0.006	Low UVB	0	0.132+0.007	High UVB	0	0.142+0.005
		12	0.141+0.009		12	0.100+0.002*		12	0.119+0.008
		24	0.105+0.006		24	0.110+0.005		24	0.115+0.003
		48	0.084+0.007		48	0.078+0.002		48	0.135+0.005*
		72	0.075+0.005		72	0.076+0.002		72	0.133+0.001*
		96	0.069+0.003		96	0.078+0.003		96	0.137+0.004*
High Temperature Low Light	Control	0	0.150+0.004	Low UVB	0	0.120+0.001	High UVB	0	0.136+0.005
		12	0.119+0.003		12	0.106+0.005		12	0.098+0.006*
		24	0.087+0.002		24	0.076+0.001*		24	0.083+0.002
		48	0.075+0.001		48	0.074+0.001		48	0.096+0.002*
		72	0.070+0.003		72	0.069+0.001		72	0.108+0.001*
		96	0.063+0.003		96	0.063+0.001		96	0.106+0.003*
Low Temperature High Light	Control	0	0.105+0.008	Low UVB	0	0.130+0.003	High UVB	0	0.111+0.011
		12	0.134+0.009		12	0.158+0.011		12	0.164+0.014
		24	0.119+0.017		24	0.136+0.010		24	0.187+0.012*
		48	0.102+0.012		48	0.093+0.002		48	0.217+0.012*
		72	0.131+0.020		72	0.131+0.004*		72	0.195+0.009*
		96	0.088+0.006		96	0.113+0.003*		96	0.161+0.009*
High Temperature High Light	Control	0	0.161+0.012	Low UVB	0	0.156+0.007	High UVB	0	0.115+0.006
		12	0.098+0.006		12	0.107+0.006		12	0.114+0.008
		24	0.114+0.008		24	0.126+0.010		24	0.205+0.015*
		48	0.089+0.005		48	0.112+0.007*		48	0.170+0.005*
		72	0.106+0.006		72	0.119+0.006		72	0.166+0.002*
		96	0.127+0.005		96	0.152+0.013		96	0.170+0.001*

Table 11. Mean (± standard error) of β-carotene Normalized to Chlorophyll *a* for All Temperature and Light Experiments. Significant Difference (p<0.05) from Control Denoted by Asterisk (*).

Environmental Conditions	UVB Treatment	Hour	β-carotene: Chlorophyll *a*					
Low Temperature Low Light	Control	0	0.0355±0.004	Low UVB	0	0.0320±0.003	High UVB	0	0.0317±0.002
		12	0.0404±0.003		12	0.0246±0.001*		12	0.0276±0.002*
		24	0.0340±0.002		24	0.0344±0.001		24	0.0286±0.001*
		48	0.0219±0.001		48	0.0204±0.001		48	0.0189±0.001*
		72	0.0236±0.001		72	0.0223±0.001		72	0.0171±0.001*
		96	0.0220±0.001		96	0.0249±0.001		96	0.0163±0.001*
High Temperature Low Light	Control	0	0.0439±0.001	Low UVB	0	0.0324±0.001	High UVB	0	0.0401±0.002
		12	0.0388±0.001		12	0.0356±0.002		12	0.0312±0.001*
		24	0.0319±0.001		24	0.0267±0.001*		24	0.0271±0.001*
		48	0.0247±0.001		48	0.0241±0.001*		48	0.0207±0.001*
		72	0.0241±0.001		72	0.0235±0.001*		72	0.0219±0.001*
		96	0.0238±0.001		96	0.0222±0.001*		96	0.0165±0.001*
Low Temperature High Light	Control	0	0.0371±0.001	Low UVB	0	0.0403±0.001	High UVB	0	0.0341±0.002
		12	0.0453±0.002		12	0.500±0.004		12	0.0485±0.006
		24	0.0297±0.008		24	0.326±0.001		24	0.0348±0.002
		48	0.0331±0.002		48	0.0294±0.001		48	0.0345±0.003
		72	0.0295±0.002		72	0.0317±0.001*		72	0.0217±0.001*
		96	0.0203±0.001		96	0.0231±0.001		96	0.0121±0.001*
High Temperature High Light	Control	0	0.0797±0.014	Low UVB	0	0.0584±0.003	High UVB	0	0.0373±0.002
		12	0.0370±0.001		12	0.0357±0.003		12	0.0316±0.008
		24	0.0321±0.009		24	0.0360±0.002		24	0.0701±0.012*
		48	0.0216±0.001		48	0.0247±0.001		48	0.0243±0.001
		72	0.0242±0.001		72	0.0242±0.001		72	0.0177±0.001*
		96	0.0270±0.001		96	0.0296±0.003		96	0.0159±0.001*

Table 12. Mean (± standard error) Fucoxanthin Normalized to Chlorophyll *a* for All Temperature and Light Experiments. Significant Difference (p<0.05) from Control Denoted by Asterisk (*).

Environmental Conditions	UVB Treatment	Hour	Fucoxanthin: Chlorophyll *a*						
Low Temperature Low Light	Control	0	0.17±0.01	Low UVB	0	0.25±0.01	High UVB	0	0.27±0.01
		12	0.22±0.01		12	0.35±0.03*		12	0.36±0.05*
		24	0.28±0.01		24	0.26±0.01		24	0.31±0.01
		48	0.37±0.02		48	0.42±0.01		48	0.34±0.02
		72	0.36±0.04		72	0.36±0.02		72	0.34±0.01
		96	0.42±0.03		96	0.39±0.03		96	0.41±0.01
High Temperature Low Light	Control	0	0.29±0.01	Low UVB	0	0.37±0.01	High UVB	0	0.32±0.01
		12	0.32±0.01		12	0.36±0.03		12	0.39±0.01*
		24	0.45±0.02		24	0.56±0.01*		24	0.52±0.02
		48	0.44±0.01		48	0.43±0.01		48	0.44±0.01
		72	0.47±0.01		72	0.49±0.01		72	0.44±0.01*
		96	0.51±0.01		96	0.52±0.01		96	0.51±0.01
Low Temperature High Light	Control	0	0.16±0.02	Low UVB	0	0.10±0.01	High UVB	0	0.22±0.02
		12	0.13±0.03		12	0.12±0.03		12	0.14±0.04
		24	0.19±0.03		24	0.13±0.03		24	0.14±0.02
		48	0.21±0.05		48	0.38±0.01*		48	0.18±0.01
		72	0.36±0.04		72	0.24±0.01*		72	0.21±0.01*
		96	0.55±0.01		96	0.48±0.02*		96	0.46±0.02*
High Temperature High Light	Control	0	0.05±0.01	Low UVB	0	0.08±0.01	High UVB	0	0.24±0.04
		12	0.21±0.01		12	0.27±0.03		12	0.27±0.02
		24	0.18±0.02		24	0.24±0.08		24	0.16±0.04
		48	0.41±0.02		48	0.32±0.03		48	0.33±0.01
		72	0.30±0.02		72	0.36±0.04		72	0.41±0.01
		96	0.38±0.03		96	0.38±0.04		96	0.39±0.01

Table 13. Mean ($\pm$ standard error) of Diadinoxanthin Normalized to Chlorophyll *a* for All Temperature and Light Experiments. Significant Difference ($p<0.05$) from Control Denoted by Asterisk (*).

Environmental Conditions	UVB Treatment	Hour	Diadinoxanthin: Chlorophyll *a*					
Low Temperature Low Light	Control	0	0.291+0.013	Low UVB	0	0.207+0.010	High UVB	0	0.202+0.006
		12	0.205+0.014		12	0.136+0.003*		12	0.163+0.014
		24	0.142+0.009		24	0.156+0.009		24	0.164+0.003
		48	0.074+0.004		48	0.071+0.002		48	0.133+0.005*
		72	0.068+0.005		72	0.068+0.001		72	0.135+0.001*
		96	0.059+0.003		96	0.070+0.003*		96	0.136+0.004*
High Temperature Low Light	Control	0	0.212+0.005	Low UVB	0	0.155+0.001	High UVB	0	0.189+0.007
		12	0.158+0.004		12	0.136+0.007*		12	0.125+0.007*
		24	0.105+0.002		24	0.093+0.001*		24	0.103+0.002
		48	0.063+0.001		48	0.063+0.001		48	0.088+0.003*
		72	0.059+0.003		72	0.057+0.001		72	0.097+0.002*
		96	0.051+0.003		96	0.052+0.001		96	0.095+0.002*
Low Temperature High Light	Control	0	0.155+0.015	Low UVB	0	0.214+0.003	High UVB	0	0.137+0.011
		12	0.223+0.023		12	0.277+0.032		12	0.299+0.049
		24	0.171+0.029		24	0.200+0.019		24	0.280+0.024*
		48	0.098+0.009		48	0.101+0.003		48	0.272+0.013*
		72	0.141+0.028		72	0.159+0.010*		72	0.200+0.005*
		96	0.075+0.005		96	0.100+0.003*		96	0.085+0.005
High Temperature High Light	Control	0	0.488+0.062	Low UVB	0	0.309+0.019	High UVB	0	0.171+0.014
		12	0.139+0.010		12	0.154+0.011		12	0.162+0.009
		24	0.183+0.013		24	0.209+0.030		24	0.661+0.171*
		48	0.087+0.004		48	0.109+0.008*		48	0.164+0.002*
		72	0.111+0.007		72	0.124+0.007		72	0.170+0.004*
		96	0.128+0.006		96	0.146+0.013		96	0.159+0.003*

Table 14. Mean ($\pm$ standard error) of Diatoxanthin Normalized to Chlorophyll *a* for All Temperature and Light Experiments. Significant Difference ($p<0.05$) from Control Denoted by Asterisk (*).

Environmental Conditions	UVB Treatment	Hour	Diatoxanthin: Chlorophyll a						
Low Temperature Low Light	Control	0	0.059$\pm$0.004	Low UVB	0	0.037$\pm$0.001	High UVB	0	0.038$\pm$0.002
		12	0.039$\pm$0.003		12	0.026$\pm$0.001*		12	0.033$\pm$0.002
		24	0.029$\pm$0.002		24	0.031$\pm$0.002		24	0.036$\pm$0.002
		48	0.015$\pm$0.001		48	0.013$\pm$0.001		48	0.028$\pm$0.001*
		72	0.012$\pm$0.001		72	0.013$\pm$0.001		72	0.022$\pm$0.001*
		96	0.011$\pm$0.001		96	0.013$\pm$0.001		96	0.029$\pm$0.001*
High Temperature Low Light	Control	0	0.042$\pm$0.002	Low UVB	0	0.035$\pm$0.001	High UVB	0	0.034$\pm$0.002
		12	0.036$\pm$0.002		12	0.029$\pm$0.001*		12	0.024$\pm$0.003*
		24	0.022$\pm$0.001		24	0.022$\pm$0.001		24	0.022$\pm$0.001
		48	0.012$\pm$0.001		48	0.011$\pm$0.001		48	0.019$\pm$0.002*
		72	0.013$\pm$0.001		72	0.012$\pm$0.001		72	0.029$\pm$0.001*
		96	0.010$\pm$0.001		96	0.011$\pm$0.001		96	0.030$\pm$0.002*
Low Temperature High Light	Control	0	0.033$\pm$0.004	Low UVB	0	0.048$\pm$0.001	High UVB	0	0.029$\pm$0.003
		12	0.044$\pm$0.006		12	0.064$\pm$0.010		12	0.065$\pm$0.013
		24	0.034$\pm$0.007		24	0.039$\pm$0.005		24	0.072$\pm$0.008*
		48	0.018$\pm$0.002		48	0.020$\pm$0.001		48	0.093$\pm$0.008*
		72	0.036$\pm$0.011		72	0.042$\pm$0.003*		72	0.116$\pm$0.013*
		96	0.014$\pm$0.002		96	0.021$\pm$0.001*		96	0.104$\pm$0.007*
High Temperature High Light	Control	0	0.084$\pm$0.012	Low UVB	0	0.055$\pm$0.004	High UVB	0	0.029$\pm$0.003
		12	0.031$\pm$0.002		12	0.031$\pm$0.003		12	0.032$\pm$0.002
		24	0.037$\pm$0.003		24	0.040$\pm$0.006		24	0.121$\pm$0.031*
		48	0.017$\pm$0.001		48	0.025$\pm$0.002*		48	0.047$\pm$0.002*
		72	0.024$\pm$0.002		72	0.028$\pm$0.003		72	0.044$\pm$0.001*
		96	0.030$\pm$0.002		96	0.041$\pm$0.005		96	0.060$\pm$0.002*

Table 15. Mean ($\pm$ standard error) of Abs_{334}/Abs_{675} for All Temperature and Light Experiments. Significant Difference ($p<0.05$) from Control Denoted by Asterisk (*).

Environmental Conditions	UVB Treatment	Hour	Abs_{334}/Abs_{675}						
Low Temperature Low Light	Control	0	1.60+0.13	Low UVB	0	1.51+0.05	High UVB	0	1.10+0.07
		12	1.72+0.07		12	1.73+0.08		12	1.98+0.02*
		24	2.38+0.11		24	2.76+0.10*		24	2.89+0.13*
		48	2.58+0.11		48	1.99+0.07*		48	3.29+0.25*
		72	1.26+0.08		72	1.30+0.09		72	1.87+0.06*
		96	1.47+0.10		96	1.71+0.05		96	1.92+0.12*
High Temperature Low Light	Control	0	1.93+0.08	Low UVB	0	2.65+0.12	High UVB	0	2.42+0.02
		12	2.33+0.04		12	2.30+0.02		12	2.19+0.04*
		24	2.35+0.06		24	2.04+0.04		24	2.24+0.04*
		48	1.47+0.09		48	1.27+0.14*		48	1.90+0.11*
		72	2.60+0.19		72	1.7+0.07*		72	2.87+0.19
		96	1.92+0.09		96	1.77+0.10		96	2.58+0.14*
Low Temperature High Light	Control	0	2.43+0.11	Low UVB	0	2.15+0.12	High UVB	0	2.21+0.13
		12	1.58+0.03		12	1.57+0.11		12	1.66+0.14
		24	1.80+0.08		24	1.68+0.09		24	2.36+0.21*
		48	1.43+0.19		48	1.32+0.12		48	2.90+0.08*
		72	2.32+0.12		72	2.69+0.12		72	6.56+0.22*
		96	1.84+0.09		96	1.89+0.06		96	5.17+0.23*
High Temperature High Light	Control	0	2.54+0.12	Low UVB	0	2.59+0.15	High UVB	0	2.94+0.15
		12	1.41+0.06		12	1.42+0.06		12	1.41+0.03
		24	2.21+0.12		24	2.59+0.11		24	2.60+0.10*
		48	2.58+0.13		48	2.74+0.13		48	3.44+0.22*
		72	1.52+0.07		72	1.42+0.02		72	2.72+0.05*
		96	1.86+0.07		96	1.72+0.04		96	3.13+0.18*